Physico-chemical characterization of urban aerosols from specific combustion sources in West Africa at Abidjan in Côte d'Ivoire and Cotonou in Benin in the frame of the DACCIWA program

Aka Jacques Adon[1], Catherine Liousse[1], Elhadji Thierno Doumbia[2], Armelle Baeza-Squiban[3], Hélène Cachier[1], Jean-Francois Léon[1], Veronique Yoboué[4], Aristique Barthel Akpo[5], Corinne Galy-Lacaux[1], Benjamin Guinot[1], Cyril Zouiten[6], Hongmei Xu[1, 7], Eric Gardrat[1], Sekou. Keita[8].

[1] Laboratoire d'Aérologie, Université de Toulouse, CNRS, UPS, Toulouse, France

[2] Centre National de Recherche Météorologique (CNRM)/Groupe d'étude de l'Atmosphère Météorologique, CNRS-Météo-France, Toulouse, France

[3] Université Paris Diderot, Unité de Biologie Fonctionnelle et Adaptative-RMCX, CNRS, UMR 8251, Paris, France

[4] Laboratoire de Physique de l'Atmosphère, Université Félix Houphouët-Boigny, Abidjan BPV 34, Côte d'Ivoire

[5] Laboratoire de Physique du Rayonnement, Université d'Abomey-Calavi, Abomey-Calavi, Bénin

[6] Géosciences Environnement Toulouse, Université de Toulouse, CNRS, UPS, Toulouse, France

[7] Department of Environmental Science and Engineering, Xi'an Jiaotong University, Xi'an, China

[8] Université de Khorogo, Khorogo, Côte d'Ivoire.

Correspondence to: adonjacks@gmail.com (J. Adon) and lioc@aero.obs-mip.fr (C. Liousse)

Abstract

Urban air pollution in West Africa has yet to be well characterized. In the frame of DACCIWA (Dynamics-Aerosol-Chemistry-Cloud Interactions in West Africa) program, intensive measurement campaigns were performed in Abidjan (Côte d'Ivoire) and Cotonou (Benin), in dry (January 2016 and 2017) and wet (July 2015 and 2016) seasons, at different sites chosen to be representative of African urban combustion sources (i.e. domestic fires (ADF), traffic (AT) and waste burning (AWB) sources in Abidjan and traffic source in Cotonou (CT)). Both the size distribution of particulate matter (PM) and their chemical composition including elemental carbon (EC), organic carbon (OC), water-soluble organic carbon (WSOC), water-soluble inorganic ions (WSI) and trace metals were examined. Results show very high PM concentrations at all sites and a well-marked seasonality as well as a strong spatial variation. The average $PM_{2.5}$ mass concentrations during the wet season are 517.3, 104.1, 90.3 and 69.1 $\mu g.m^{-3}$ at the ADF, CT, AT and AWB sites, respectively. In the dry season, $PM_{2.5}$ concentrations decrease to 375.7 $\mu g.m^{-3}$ at the ADF site, while they increase to 269.7, 141.3 and 175.3 $\mu g.m^{-3}$ at the CT, AT and AWB sites, respectively. The annual $PM_{2.5}$ levels at almost all sites are significantly higher than the WHO guideline level of 10 $\mu g.m^{-3}$. As for PM mass, (EC) and (OC) concentrations are also maximum at ADF site, accounting up to 69% of the total PM mass. Such high content is mainly linked to wood burning for domestic cooking and commercial food smoking activities. Dust contributions are dominant at CT (57-80%), AT (20-70%) and AWB (30-69%) sites and specially in the coarse and fine particle modes at CT and in the coarse fraction at AT site, which may be explained by the impact of long-range desert-dust transport and re-suspended particles from the roads, in addition to anthropogenic sources. The contributions of WSI to the total PM mass, mainly driven by chloride, nitrate and calcium in the fine and/or large particles are highly variable according to the sites but remain less than 30%. Values are generally 1-3 times higher in the wet season than the dry season. This is due to anthropogenic emissions but also to nitrate formation by reaction processes and natural emissions. The concentrations of trace element well reflect the trends of dust at the traffic and AWB sites, with a predominance of Al, Na, Ca, Fe and K, keys markers of crustal dust. This study constitutes an original database that characterizes specific African combustion sources.

Keywords: atmospheric pollution, chemical composition, physicochemical characterization, Particulate matter, traffic, waste burning, domestic fires.

1. Introduction

The impact of anthropogenic pollution on environment and health has been demonstrated by numerous studies in Europe and North America, which have contributed to the implementation of emission reduction policies. By contrast, air pollution in Africa is far from being well characterized, although it is suspected to be responsible for negative health outcomes (*WHO, 2014*). This is a major problem since Africa is an intense emitter of pollution from anthropogenic sources that includes domestic fires, vehicular traffic, waste burning as well as growing oil and mining industries. It has also one of the fastest growing urban populations in the world, especially in West and East Africa (UN, 2019). As a consequence, it has been shown that massive urbanization and rapid economic growth could be responsible for tripling anthropogenic emissions in Africa between 2000 and 2030 (*Liousse et al., 2014*). Moreover, it is important to recall the impact of biomass burning and dust sources in the African atmospheric composition, especially occurring during the dry season. All of this results in a major degradation of urban air quality and an impact on the health of exposed populations. Only a few studies on this subject have been conducted in West Africa (*Val et al., 2013*; *Dieme et al., 2012*; *Kouassi et al., 2009*) despite the high atmospheric pollutant concentrations already measured to be of the same order as in Asian megacities and well above WHO international standards (*WHO, 2014*).

West Africa is then an "unique laboratory" to study urban pollution. Previous studies conducted under the framework of the AMMA (Analyses Multidisciplinaires de la Mousson Africaine) and POLCA (POLlution des Capitales Africaines) programs, have revealed very high average particulate mass concentrations in Cotonou (Benin), Bamako (Mali), Dakar (Senegal) and Yaoundé (Cameroun) during the dry season (*Doumbia et al., 2012; Val et al., 2013*), suggesting that the population may be affected by negative health outcomes. For example, during the dray season in Bamako (Mali) and Dakar (Senegal), *Val et al. (2013)* showed that the inflammatory impact of combustion aerosol depends on the type of emission sources and determined the predominant role of particulate organic matter. This is consistent with global findings showing that fine and ultrafine aerosol fractions, as well as their content in trace metals and organic compounds, induce biological effects due to their ability to reach the distal lung (*Cassee et al., 2013*). Such reasons highlight the need to better understand the size-speciation of aerosol chemical composition for the main West African anthropogenic sources during the different seasons. Within this context, the DACCIWA (Dynamics-Aerosol-Chemistry-Cloud Interactions in West Africa) program, dedicated a specific work package to “Air Pollution and

Health" dealing with pollutant characterization related to health issues through toxicological studies and epidemiological studies.

Campaigns have been organized from December 2014 to March 2017 in Abidjan and Cotonou. The strategy was to measure aerosol chemical composition in different sites, representative of the main prevailing urban sources in West Africa following *Liousse et al. (2014)* and *Keita et al. (2018)*. Two typical traffic-sampling sites were chosen, one in Abidjan (Côte d'Ivoire) and another one in Cotonou (Benin), to take into account differences in terms of fleets, type of fuel used and quality of roads. Indeed, in Cotonou, the majority of population uses two-wheel vehicles susing gasoline fuel or gasoline and oil fuel, whereas in Abidjan, the vehicle fleet is dominated by four-wheel engines using diesel fuel. Measurements were also performed at domestic fire and waste burning sites, both located in Abidjan.

For a period of two years, $PM_{2.5}$ mass and carbonaceous aerosol were weekly measured and results are discussed in *Djossou et al. (2018)*. In this paper, we focus on the results from the intensive campaigns. We present measurements obtained at each site during the wet and dry seasons of the studied periods: (i) PM size distribution and mass concentrations and (ii) PM chemical composition including carbonaceous aerosol, water-soluble organic carbon, water-soluble inorganic ions, dust and trace elements in different size fractions. Experimental method including description of sites, types of measurements and analyses, meteorological conditions, will be presented in the section 2, whereas results and discussion are discussed in the sections 3 and 4 of the paper, respectively.

2. Experimental method

2.1. Description of sites

Measurement campaigns have been performed in wet season (July 20-26, 2015 and July 4-13, 2016) and dry seasons (January 7-15, 2016 and January 5-14, 2017) at three sites in Abidjan (Côte d'Ivoire), representative of different sources, i.e. ADF for Abidjan Domestic Fires, AWB for Abidjan Waste Burning and AT for Abidjan Traffic (Figure 1), as well as one traffic site in Cotonou (Benin) (Figure 2).

As shown in Figure 3 which presents pictures of the different sampling sites, the ADF site (5˚ 19' 44 "N, 4˚ 06' 21" W) is situated on a platform, 5 m above ground level, in Yopougon

Bracody district near a market (Figure 1). This geographical area is highly populated with various small commercial activities such as a fish and meat-smoking by women. There are also many formal and informal settlements, which mainly use wood and charcoal as a source of fuel for private and professional combustion activities. Other sources of concern contributing to the mix of pollutant emissions in the area include transportation-related emissions, biomass burning, garbage bins or small landfills and various other fugitive sources. The AT site (5° 21' 14" N, 4° 01' 04" W) is located in Adjamé, on the roof of « 220 pharmacie logement building », about 7 m above ground level and roughly 10 m away from the main road. This site, close to the Adjamé market and to a bus station, is highly affected by traffic (Gbaka, bus, taxi, woro-woro, private cars…). The AWB site (5° 21' 12" N, 3° 56' 16" W) is located at Akouédo in the district of Cocody, on the roof of « Talafiguié », a building 15 m above ground level. This site close to the big municipal landfill of Abidjan operational since 1965 and now covering an area of 153 ha, is submitted to frequent waste burning pollution. The Cotonou Traffic (CT) (6° 22' 19" N, 2° 26' 5" E) site is located in Cotonou, on the «Sogema» building roof, about 7 m above ground level. This site is close to the Dantokpa market and also to the biggest crossroad of Cotonou (intersection of 4 main roads). This site is highly influenced by intense traffic activities. As previously mentioned, such a site is interesting because the vehicle fleet and fuels are different in Cotonou compared to Abidjan: (1) there are many two-wheel vehicles in Cotonou whereas a few only in Abidjan; (2) in Cotonou, gasoline is of poor quality due to the illegal fuel transport from Nigeria and (3) the roads are in worse conditions in Cotonou than in Abidjan.

2.2. Measurements

During each intensive campaign and on each site, two 3-hour samples collected with cascade impactors operating in parallel are obtained for three consecutive days (i.e. six size-resolved samples per site during each campaign), to allow size-speciated characterization of the aerosol chemical composition. Note that the choice of the 3-hour periods is linked to the period of maximum pollution for each site as shown by preliminary studies (e.g. morning at ADF site (7-10am), afternoon at AT site (4-7pm, morning at CT site (7-10am)). There is no specific period at AWB site since the activities are roughly the same during the day. The first impactor with 4 stages ($PM_{>2.5}$; $PM_{2.5-1}$; $PM_{1-0.2}$; $PM_{<0.2}$) includes 4 quartz fiber filters (QMA, Whatman) for mass and carbonaceous aerosol (EC, OC and WSOC analysis). The second impactor with 3 stages ($PM_{>2.5}$; $PM_{2.5-1}$; $PM_{1-0.1}$) is equipped with three Teflon filters (Zefluor, Pall Corporation®), dedicated for water-soluble ions species and trace elements. Due to operational

problems in july 2016, this second 3-stage cascade impactor is replaced by another 3-stage cascade impactor with different size cuts ($PM_{>10}$, $PM_{10-2.5}$, $PM_{2.5-1}$). For consistency, results will be presented as an ultrafine (UF), fine (F) and coarse (C) classification. The two first stages ($PM_{>2.5}$ and $PM_{2.5-1}$) being considered as the coarse particulate fraction, the $PM_{1-0.1}$ or $PM_{1-0.2}$ stage, the fine particulate fraction and the $PM_{<0.2}$ stage, the ultrafine fraction.

All the filters are prepared and analyzed at the Laboratoire d'Aerologie in Toulouse under different protocols described in the following paragraphs. Note that the quartz filters are prefired before sampling.

2.3. Analyses

2.3.1. Gravimetric analyses

Aerosol mass concentrations are obtained using a high-precision balance (SARTORIUS MC21S), placed under a controlled temperature and humidity atmosphere (Person and Tymen, 2005). Before weighing, the filters are kept 24 hours in the weighing room at an ambient relative humidity of 30 ±15%. The filters are weighed before and after sampling. Result of a gravimetric measurement consists of the average of 2 to 4 weighing whose differences do not exceed 5µg. The standard error on a gravimetric measurement is therefore less than 10 µg, typically representing less than 5% of the particles mass.

2.3.2. Carbonaceous aerosols

Carbonaceous aerosol is determined with thermal analysis with a two-step method adapted from Cachier et al. (1989). Two aliquots of the same filter are separately analyzed.

One portion is directly analyzed for its total carbon content (TC). The other portion is first submitted to a pre-combustion step (2 h at 340°C under pure oxygen) in order to eliminate Organic Carbon (OC), and then analyzed for its Elemental Carbon (EC) content. Organic carbon (OC) concentrations are calculated as the differences between TC and EC. Note that the aerosol carbon content is quantified by a non-dispersive infrared (NDIR) detector with G4 ICARUS instrument with a detection limit of the order of 2 $\mu gC.cm^{-2}$. Uncertainty is in the order of 5% for TC, while being in the range of 5-20%, for EC and OC.

2.3.3 Water Soluble Organic Carbon analysis

WSOC measurements are performed using a total organic carbon analyzer (Sievers M9). A detailed description of this technique is reported in Favez et al. (2008). Briefly, the full

oxidation of total organic carbon into CO_2 is obtained by coupling chemical oxidation (with ammonium persulphate) and UV light. CO_2 is then quantified by conductivity. Analyses are conducted on 20 ml of solution extracts. For UF samples, solutions to be analyzed are obtained using a total filter surface of 3cm² (6x0.5 cm² punches symmetrically taken out of each QMA filter), whereas, for C and F sizes, due to the geometry of the spots at the surface of the filters, samples are divided into equivalent parts (1/2 or 1/4 of 47 mm filters, rest of the filters being used for carbonaceous analysis). The extraction protocol consists of 16h soaking under soft shaking in an Erlen-Meyer containing 20mL of ultra-pure water. Prior to WSOC analysis, water extracts are filtered through Teflon (PTFE) filters (0.2µm pore size diameter) in order to remove any suspended particle. Measurement uncertainty, given by the manufacturer, is of the order of 7%. The overall calculated blank value is of the order of 2.27 ± 0.33 µgC.cm^{-2}, which represents 16.4± 8.5% of the mean WSOC content. For each sample, duplicate analyses show a good reproducibility.

2.3.4. Water-soluble ionic species

Water-soluble ionic species (Na^+, NH_4^+, K^+, Mg^{2+}, Ca^{2+}, SO_4^{2-}, NO_3^- and Cl^-) are analyzed using ion chromatograph (IC), following the analytical protocol described in Adon et al. (2010). Briefly, the aerosol water-soluble fraction is first extracted from half-sampled Teflon filter (the other part being used for trace element analysis), with a 10-min sonication in plastic vials including 6 ml or 10 ml of purified water with a controlled resistivity of 18.2MΩ. Then these vials are subjected to ionic chromatograph analysis or stored at +4°C if not analyzed immediately. Cations are analyzed with Dionex DX-100 and anions with Dionex DX-500 with a detection limit of 1 to 6 ppb depending on ionic species. Uncertainties in the range of 1-50% is found depending on ionic species.

2.3.5. Trace elements

The protocol to measure trace element concentrations is developed and performed at the Laboratory of Environmental Geosciences of Toulouse. Half-sampled Teflon filters (the other part being used for water-soluble ionic species, see below) are mineralized by acid digestion with a 10 ml concentrated HNO_3 and 0.5 ml HF solution (Lamaison, 2006) using a closed vessel microwave accelerated reaction system (MARS 5, CEM Corporation) at high pressure (700 psi) (Celo et al. 2010). The digestion is realized in 3 steps: a rise in temperature at 130°C in 3min and holding for 1 min, then, a second rise at 160°C in 1 min and holding for 30 seconds and finally a third rise to 180°C in 1 min and holding for 3min. After a 12 h cooling period, the

solutions are evaporated at 80°C, and concentrated in 7 ml of 2% concentrated HNO_3 solution, before analysis by ICP-MS which are performed with a 7500 ce Agilent Technologies instrument equipped with a collision cell, and using In and Re as internal standards. The detection limit is less than 10 ppt. For all the samples, the final blank values and detection limit on filters are taken into account for final concentrations calculations. 13 trace metals are considered in this work: Al, Ti, Cr, Mn, Fe, Ni, Cu, Zn, Ba, La, Th, Pb and Cd.

2.3.6. Dust calculation

Many methods can be used to quantify dust concentrations. We have selected three methods (Sciare et al. 2005, Guinot et al. 2007, Terzi et al. 2010) to underline the uncertainties linked to dust estimates.

(1) Sciare et al. (2005) method consists of using soluble calcium data obtained with Ionic Chromatography (IC), to estimate the dust concentrations following the relationship: dust = 10.96*nss-Ca^{2+}, where nss-Ca^{2+} (=1.02*Ca^{2+}-0.038*Na^{+}) refers to non-sea-salt calcium concentration.

(2) Guinot et al. (2007) method is based on a chemical closure where fine and coarse particle aerosols are separated in 4 components (EC, POM, WSI and dust). EC, WSI, and total aerosol mass are directly experimentally determined (see below paragraphs). POM concentrations are obtained from OC concentrations experimentally determined and k, the OC/POM conversion factor. Dust concentrations are obtained from measured Ca^{2+} concentrations and f, the abundance of calcium in dust. The k and f values are obtained from a linear regression (L) between the reconstructed and the weighed aerosol mass concentrations. Briefly, first step consists of focusing on the aerosol coarse fraction. k is fixed to 1.8 and as a result of (L) just mentioned, f is obtained to be in the range of 0.012 to 0.15 depending on our sites. Second step deals with the aerosol fine fraction. The f values just obtained for the aerosol coarse fraction are applied to the fine fraction and k ratios are estimated using (L) to be in the range of 1.2 to 2.1. Note that at all of our sites, the correlation between Ca^{2+} and the missing mass between the weighed and the reconstructed aerosol mass is sufficiently good (r^2=0.9) to support the consistency of this simple approach for the evaluation of dust. Also, f and k values are included in the range of values provided in the literature (He et al. 2001; Sun et al. 2004; Guinot et al. 2007). However, it is important to mention that the range of f and k coefficients are large which is due to the source mixing observed in this study.

(3) In Terzi et al. (2010) method, dust is obtained with the following relationship: dust = 1.89[Al] + 1.21[K] + 1.95[Ca] +1.66[Mg] + 1.7 [Ti] +2.14[Si] + 1.42[Fe]. In our study, all these elements are determined except Silica (Si). Consequently, we used mean Si values obtained from different relationships available in the literature ($SiO_2 = 3*Al_2O_3$ for Alastuey et al., 2005, Si = 4.0*Al for Zhang et al., 2003 and Si = 2.03*Al for Chiapello et al., 1997).

The results of dust concentrations estimated from the three methodologies above described are summarized in the Table 1 for wet season (WS) 2016 and dry season (DS) 2017. Indeed, Ca, Al, and Fe concentrations measured by ICP-MS are only available in WS2016 and DS2017 due to experimental problems, whereas Ca^{2+} concentrations measured by IC are available for all campaigns. As shown in table 1, the dust obtained from Ca^{2+} measured by IC (Sciare et al., 2005) and by the Guinot et al. (2007) method is lower than that obtained from trace elements (Terzi et al., 2010) for DS2017 whereas in the same order of magnitude in WS2016. Such results are in agreement with methodological aspects. Indeed, Al, Fe, Ca … obtained by ICP-MS include both soluble and insoluble particles whereas Ca^{2+} measured by IC only include soluble particles. During the dry season, comparison of Ca measured by ICP-MS (not shown here) is higher than that of the IC, by a factor of 1.7, 1.8, 2.2 and 1.1, at the ADF, AWB, AT, and CT sites respectively. By contrast, this factor is low and constant (1.3) in the wet season for all the sites. In our study, due to the lack of trace element data for WS2015 and DS2016, dust estimations are performed from Guinot et al. (2007) method. This choice globally implies an underestimate of dust concentrations by a factor of 1.5 to 3.5 in DS2017 as shown in Table 1.

2.3.7. Aerosol chemical closure methodology

As previously mentioned and detailed, aerosol chemical closure is performed following the Guinot et al. (2007) methodology.

2.4. Meteorological conditions

In Figure 4, meteorological data (surface temperature, wind directions and speed) issued from the NOAA Integrated Surface database (ISD; see https:// www.ncdc.noaa.gov/isd) and the ASECNA (Agence pour la Sécurité de la Navigation Aérienne en Afrique et à Madagascar) are presented for the South-West Africa region including Abidjan and Cotonou. As expected, this

area is under the influence of the Convergence Zone of two air masses of a different nature, i.e. Harmattan (hot and dry continental trade winds) from the north and Monsoon (humid maritime trade winds) from the south (Figure 4). Ground contact between these two air masses constitutes the intertropical front (ITF) of which the fluctuations during the year determine the seasons in the Gulf of Guinea (Tapsoba, 1997). During the dry season (from November to March), temperatures are relatively high with maximum around 30°C on the coast. The humidity is low, since the prevailing Harmattan wind blows from the desert, usually bringing dust (Figure 4, lower line). The period from June to September, especially in July is the wet season period when daytime temperatures are slightly lower, with maximum around 26/28°C on the coast (Figure 4, upper line). At this season, the humidity level is high across the region. On the coast, rains may occur from March to November.

During our campaigns (not shown here), temperatures are roughly the same at Abidjan and Cotonou, reaching 28°C and 26°C in the dry and wet seasons, respectively. Gentle to moderate wind speeds are observed during the measurement campaigns at the two cities, with average values of 15-20 and 15-22 $km.h^{-1}$ at Abidjan and Cotonou, respectively. There is no precipitation at CT site during the studied periods. In Abidjan on the contrary, low rains occur both in wet and dry periods with cumulative precipitation higher in DS2017 (7mm), than in WS2016 (4.7mm) and WS2015 (2mm). There is no rain in DS2016 (https://www.historique-meteo.net/afrique/).

2.5. Backward trajectories

The Hybrid Single-Particle Lagrangian Integrated Trajectory (HYSPLIT) modelling system (Air resources laboratory, Draxler and Rolph, 2012) is used for the trajectory analysis. HYSPLIT model is run to compute 120 h back trajectories ending at Abidjan and Cotonou at 50 m a.g.l. (Figure 5). Global Data Assimilation System reanalysis database is used as meteorological input, with a 0.25 × 0.25 degrees horizontal resolution. Results presented in Figure 5, confirm that air masses mainly come from the north with a few from the south-west in dry season (January), whereas from the south-west and the south in wet season (July). Therefore, in January, Abidjan and Cotonou are mainly impacted by polluted air masses from surrounding areas and northern countries with possible dust and west African biomass burning influences, whereas in July, the impact of oceanic sources possibly polluted by long-range south African biomass burning aerosols may be observed.

3. Results

3.1. Aerosol size distribution and mass concentration

In Figure 6, the relative mass distribution of PM for Coarse (C), Fine (F) and Ultra-Fine (UF) particle sizes in percentages are presented with bulk mass concentration averages indicated in the black boxes for each site and for each campaign. As it may be seen, bulk concentrations vary widely from site to site and from campaign to campaign. During the wet season, the average total concentrations range from 82 to 676 $\mu g.m^{-3}$ in 2015 and 56 to 358 $\mu g.m^{-3}$ in 2016, with the maximum at the Abidjan Domestic Fire (ADF) site. While during the dry season, values range from 168 to 269 $\mu g.m^{-3}$ in 2016 and from 114 to 559 $\mu g.m^{-3}$ in 2017, with maximum concentration obtained at the Cotonou Traffic (CT) and ADF sites. In terms of size distribution, concentration peaks may be observed for all aerosol size-fractions which are found to exhibit different seasonal patterns. UF particles (<0.2 µm) represent the highest contributor to the bulk mass at the ADF site, by up to 60 % (335.3 $\mu g.m^{-3}$) in DS2017. F particles (1-0.2 µm) are the second most important contributor and both combined particle sizes account for more than 85 % of the total mass at the ADF site. In this site, ultra-fine and fine fractions are also found to be maximum during WS2015 and WS2016 by up to 90 and 83%, respectively. Let us note that C particle contribution in bulk is relatively higher in the traffic and waste burning sites than in ADF site (40%) whereas F and UF particle contributions are on the order of 60%.

In terms of PM2.5, the results of this work are presented in Figure 7. The mass concentration of PM2.5 averaged over DS2016 and DS2017 are 154 ± 74, 144 ± 42, 134 ± 7 and 211 ± 51 $\mu g.m^{-3}$ at the ADF, AWB, AT and CT sites, respectively and 338 ± 24, 45 ± 3, 52 ± 4 and 70 ± 1 $\mu g.m^{3}$ over the wet seasons (2015-2016). The increase in PM2.5 is of the order of 54% at ADF from dry to wet season, whereas a sharp reduction (more than 60%) is obtained at AWB, AT, and CT sites.

3.2. Carbonaceous aerosol

3.2.1. EC and OC concentrations

In Figure 8, EC relative mass contributions are presented for each size, site and campaign: wet season 2015 (WS2015), wet season 2016 (WS2016), dry season 2016 (DS2016) and dry season 2017 (DS2017). Mean EC bulk mass concentrations are added in the black boxes for each size and for each campaign. The most striking feature is that the ADF site concentrations are higher than at the other sites in WS2016 and in DS2017, whereas of the same

order of CT site concentrations in the other seasons. Mean concentration at the CT site (16µg.m^{-3}) is slightly higher than at the AT site (10µg.m^{-3}), whereas the lowest concentrations are found at the AWB site. Results of the EC size distribution are very consistent among the different sites (Figure 8). Whatever the site and the season, higher EC concentrations are found in C (42%) and UF (43%) particles compared to F particles.

Same data are presented for OC concentrations in Figure 9. It may be underlined that ADF OC values are always higher than in the other sites by a factor ranging from 6 to 30, for all seasons and particle sizes, with highest and lowest values respectively in DS2017 and DS 2016. In terms of size distribution, maximum OC concentrations at the ADF site may be found in UF (53%), then F (29%) and finally C (18%) particles. The same distribution is observed for the traffic sites in DS2016, however, for the other campaigns, OC size distribution looks like the EC ones with higher concentrations in UF and C particles than in F particles.

As shown in Figure 10, the highest OC/EC ratios are always obtained at the ADF site with a value as high as 25 for F particles in WS2016 whereas the lowest values are found in DS2017. This is the same feature for the other sites with ratios lower than 2 in DS2017. OC/EC ratios in AWB site are higher than in the traffic sites. Note that values at AT site are higher than CT values in the wet season whereas lower in the dry season. Finally, it is interesting to underline that linear correlations between EC and OC are obtained in the ultrafine and fine modes in all campaigns, particularly in DS2017 (r^2 = 0.8, 0.8, 0.9 and 0.9) at the ADF, AWB, AT and CT sites, respectively. This suggests that different studied sources can be assessed as significant sources of both EC and OC.

3.2.2. Water-Soluble Organic Carbon

Concentrations of WSOC and WSOC/OC ratios are presented in Table 2 for each size (UF, F, C and PM2.5) and campaign. As seen, WSOC are always higher at the ADF site than in other sites, at least by a factor of 12. Maximum values are obtained in WS2016 with an average of 16.47, 17.08 and 79.68 µgC.m^{-3} for coarse, fine and ultra-fine fractions, respectively, followed by WS2015 and DS2017. WSOC concentrations are the lowest in DS2016, with an average of 4.14, 6.95 and 21.89 µg.m^{-3} for coarse, fine and ultrafine fractions, respectively. In terms of seasonality, there is not a clear trend in WSOC values at the AWB and AT sites, whereas at the CT and ADF sites, WSOC values are found to be respectively higher and lower

in dry seasons compared to wet seasons. It is also interesting to note that WSOC are maximum in UF sizes in the AT, ADF and AWB sites. At the CT site, the highest values are found in the coarse particulate fractions, except in DS2016.

As expected, WSOC is strongly correlated with OC (r=0.7 at ADF, 0.8 at AT, 0.5 at AWB and 0.7 at CT), whereas correlations with EC are weaker, especially at the AWB and CT sites with values ranging from 0.1 to 0.4, respectively. Finally, when looking at WSOC/OC ratios (Table 2), maximum values are obtained at the ADF site with PM2.5 ratios as high as 43%, followed by the AT and AWB sites with 32%. The lowest value (23%) is found at the CT site. Also, Table 2 shows that there is no clear seasonality in WSOC/OC values, excepted at ADF where maximum values occur during the wet season. Note as for WSOC, that ratios are maximum in UF and F fractions for all sites except at the CT site where the ratio for coarse fraction is the highest.

3.3. Water-soluble ionic species

Figure 11 shows the relative contribution of the major ions to the total concentration (also given) of the ions in the different particle modes (C and F) at the ADF, AWB, AT and CT sites for the different measurement campaigns. Let us recall here that only C and F fractions may be documented due to the our experimental protocol. Total concentrations present maximum values in ADF and CT sites. Values in AWB and AT sites are of the same order of magnitude and lower by a factor of 2 than in ADF and CT sites. The contribution of different ions show significant variations from site to site. The dominant ionic species at the ADF site over all campaigns is chloride (Cl^-), with a 26% contribution, followed by nitrate (NO_3^-) (16%), calcium (Ca^{2+}) (13%) and potassium (K^{2+}) (12%). Sulfate (SO_4^{2-}), ammonium (NH_4^+), sodium (Na^+) and to a lesser extent magnesium (Mg^{2+}) contributions are lower, ranging from 4 to 7% of the total ion species. The lowest contribution is for organic acids with their total value lower than 5%. NO_3^- is the major ionic component at the AWB and AT sites, representing 24% and 29% of the total water soluble inorganic concentration, respectively. The second major contributor in AWB and AT is SO_4^{2-}, accounting for 21% and 17% of the ion mass, respectively followed by Ca^{2+} (12% and 15%) and Cl^- (15% and 13%). In CT, Ca^{2+} is predominant with a relative abundance of 24%, followed by NO_3^- (23%), SO_4^{2-} (19%) and Cl^- (13%). Na^+, NH_4^+ and K^+ contributions are lower and in the same order of magnitude in AT, AWB and CT sites, ranging from 4 to 9% of the total ion species. Note that organic ion contributions at AT, CT and AWB is of the same order than in ADF, with lower values at CT. It is interesting to underline in the Figure 11, that NO_3^- contribution is always higher in the coarse than in the fine size.

Conversely, K^+ is always higher in the fine than in the coarse size. In CT, Ca^{2+} in the fine fraction is as high as in the coarse fraction whereas in AT, AWB and ADF, Ca^{2+} coarse fraction is predominant. Fine particle contribution may be noticed for Cl^- in ADF whereas in the other sites, Cl^- is most likely dominated by coarse particles. Finally, SO_4^{2-} is mainly found in the fine mode at the AT, AWB and CT sites, but in the coarse mode in ADF site.

In terms of seasonal variations, it may be shown in Figure 11 that higher Cl^- values are found in wet seasons than in the dry seasons everywhere, except in ADF site where there is no marked difference between seasons. For example, the mean relative total percentages of Cl^- at the CT site are 38 and 24% in the WS2015 and WS2016, respectively, while these percentages decrease significantly to 18 and 13% in the DS2016 and DS2017, respectively. The Cl^-/Na^+ ratios are about 1.5 everywhere in both seasons, in agreement with the typical sea water ratio (1-1.2) (Hara et al.,2004), except at the ADF site where these ratios increase to 4 and 5 in wet and dry season, respectively and at the AWB site in the dry season (2). K^+ and Ca^{2+} are always higher in dry season than in wet season except for Ca^{2+} in ADF where values are of the same order. Finally, the same trend is observed for NO_3^- and SO_4^{2-} with higher values in dry than in wet seasons at AWB and CT sites whereas values at ADF and AT sites are of the same order of magnitude for the two seasons.

3.4. Trace element concentrations

Table 3 shows the mean values of the major trace elements in bulk aerosol at the different studied sites in WS2016 and DS2017, with their corresponding relative abundances in the total aerosol mass into brackets. Let us recall that data are not available in WS2015 and DS2016. The concentrations of trace elements span a wide range, from 0.2 to 25.2 $\mu g.m^{-3}$. Among the measured elements, Al, K, Na and Ca are the most abundant, followed by Fe and Mg. In DS2017, Al and Na concentrations are higher in AWB than in the other sites. The minimum value for these species is found in ADF site. Values in traffic sites are of the same order of magnitude and higher than in ADF site. Maximum of Ca and K values may be found in CT and ADF site respectively. It is interesting to note that Al, K, Na concentrations are higher in the dry season than in the wet season. Such feature is less clear for Ca, whose seasonal variability is less marked except in AWB and AT sites. In terms of Mg, maximum values are observed in ADF site and of the same order of magnitude whatever the season. Fe abundance is higher in AWB and CT sites than in ADF and AT sites and higher in DS2017 than in WS2016 everywhere. The other metals (Ti, P, Zr, Zn, Cr, Mn, Pb and Ni) represent less than 0.5% and

445 2% of the total mass in WS2016 and DS2017, respectively, at all sites, with Cr, Mn, Pb and Ni
446 exhibiting less seasonal variability compared to the rest of the metal elements.
447 To assess the relative contribution of crustal and non-crustal origin of elemental aerosol
448 loadings, source enrichment factor (EF) of a trace element X have been first calculated with the
449 following formula using both literature data of the typical elemental composition of the upper
450 continental crust (Mason and Moore, 1982; Taylor, 1964), measured elemental composition
451 from this study and Al as a reference element :

452 $$EF_X = \frac{\frac{[X]_{atm}}{[Al]_{atm}}}{[X]_{soil} / [Al]_{soil}}$$

453 Where $[X]_{atm}$ and $[Al]_{atm}$ are the concentrations of the chemical element X and Al in the
454 atmosphere, respectively, and $[X]_{soil}$ and $[Al]_{soil}$ are the typical concentrations of the element
455 X and Al in the earth's crust, respectively. Al is frequently used as a reference element assuming
456 that its anthropogenic sources in the atmosphere are negligible (Gao et al., 2002; Cao et al.,
457 2005; Xu et al., 2012). In all sampling sites, EF values typically lower than 5 are obtained for
458 several trace elements (Be, Sc, Ti, V, Fe, Ga, Sr, Nb, Rh, Ba, La, Ce, Pr, Nd, Sm, Eu, Gd, Tb,
459 Dy, Ho, Er, Tm, Yb, Lu, Ta, Th and U). This suggests a natural origin of these species (Freitas
460 et al., 2007; Gao et al., 2002). The most enriched elements (EF>100) are Sb, Sn, Zn, Se, Te,
461 Cd, Pb, Bi and Mo at nearly all of the sites, indicating significant anthropogenic origin (Wang
462 et al., 2006). These elements are mainly emitted into the atmosphere through fossil fuel
463 combustion, traffic emission, wear of brake lining materials and industrial processes (Watson
464 and Chow, 2001; Samara and al., 2003). Secondly, source contributions have been estimated
465 from these EF values following the method described by Arditsoglou and Samara (2005). Note
466 that this study refers to ratios for a limited list of sources, perhaps not including the African
467 source specificities. As a result, it may be seen that 30% of trace element concentrations is of
468 anthropogenic origin at ADF site whereas about 17 % at the others sites.

469 **3.5. Dust**

470 Figure 12 shows dust concentrations calculated from Guinot et al. (2007) methodology
471 (see paragraph 2.3.6) for C and F particle sizes at the different sites for each season. Note that
472 as for WSI and trace element and due to our sampling procedure, there are values for fine and
473 coarse particles for all seasons excepted for WS2016 with values for coarse particles only.
474 During the wet season, coarse dust concentrations range from 5 to 25 $\mu g.m^{-3}$ in 2015 and 9 to
475 37 $\mu g.m^{-3}$ in 2016, with higher values at the CT and ADF sites in 2015 and at AT, CT and ADF

in 2016. In WS2015, fine dust concentrations range from 12 to 49 with maximum values at ADF and CT sites also. During the dry season, values range from 38 to 156 $\mu g.m^{-3}$ in 2016 and from 41 to 116 $\mu g.m^{-3}$ in 2017, with maximum concentrations obtained at the CT site, followed by AWB site. When considering mean values of the dry seasons, total dust at CT is 2.4 times the values found at AT, 1.6 times at AWB and 3.4 times at ADF. Seasonal comparison shows that total dust concentration is higher in the dry seasons than in WS2015 by a factor of 3 in AT, 2.6 in CT and 4 in AWB, but of the same order of magnitude in ADF site.

3.6. Aerosol chemical closure

The aerosol chemical closure obtained using the Guinot et al. (2007) method (see below) at the different sites for each season is presented in Figure 13. Results show clear intra- and inter-annual variations at all of the sites, as well as significant differences among the sites. In total, dust accounts for 39 to 75% of the bulk PM mass at both traffic sites, with no clear seasonal cycle and higher contributions in Cotonou (Figures 13c and 13d). These percentages vary from 32 to 64% at the AWB site, and from 18 to 35% at the ADF site, with percentages 1.8 times higher in the dry season than in the wet season in AWB and no clear seasonal difference in ADF (Figures 13a and 13b). Carbonaceous aerosol, the sum of EC and POM, show large contributions at the ADF site (from 49 to 69% of the total PM mass), with relatively similar proportions in each season (Figure 13a). The absence of a clear seasonal pattern is also observed in CT whereas carbonaceous aerosol is slightly higher in WS than in DS in AWB (23 and 16% respectively) and AT (37 and 21% respectively) (Figures 13b-d). Carbonaceous aerosol contribution accounts for about 11- 49% of the total mass at both traffic sites with higher values in AT (mean of 30%) than in CT (13%). The ion percentages in PM fractions present the same pattern at AT, CT and AWB sites with higher values in wet than in dry seasons. In these sites, we may notice that mass concentration in coarse particles is larger in the wet season whereas of the same order of magnitude than the one in fine particles in the dry season. In ADF, no marked difference may be found between the seasons and the sizes (Figure 13).

4. Discussion

A discussion of the results site by site (Abidjan domestic fire site, traffic sites both together and waste burning site) will be first proposed. We will scrutinize (1) the proximity between the sites and the sources; (2) the source specificity with more or less incomplete combustion (e.g. wood combustion and two-wheel vehicle emission factors are higher than gasoline emission factors

(Keita et al., 2018); (3) the relative influence of other local sources or transported sources to the studied sites such as dust and biomass burning; (4) the occurrence of continental air masses; (5) the variation of the boundary layer height (as reported by Colette et al., 2007); and (6) the meteorological parameters (e.g. temperature, relative humidity and wet deposition) to explain the differences of pollutant concentrations and their seasonal and inter-annual variabilities.

In a second part, we will present comparison of our values with other DACCIWA values and also with literature values for other intensive campaigns in Africa.

4.1. Abidjan Domestic Fires (ADF)

As shown in the above paragraphs, maximum values are obtained at the ADF site, for aerosol mass, EC, OC, WSOC, water-soluble ionic species (e.g. Cl^-, NO_3^-, Ca^{2+} and K^+) and some trace elements such as Mg and K (whereas Al, Na and Fe are lower than in the other sites). Also, aerosol PM2.5 values are well above the annual and daily WHO guidelines of 25 and 10 $\mu g.m^{-3}$ respectively, whatever the season.

Such pattern is due to the proximity of the ADF site to the studied combustion source: in that area, the use of wood combustion is very active due to commercial activities of women drying fish and meat and domestic cooking. This is also confirmed by the high relative importance of total carbon in aerosol mass whatever the size (49 to 69%) and by values of source enrichment factor. Indeed, at least 30% of trace element concentrations are of anthropogenic origin at ADF site. In addition, wood combustion is well known to be highly polluting due to incomplete combustion: this is shown here by the measurements of very high OC/EC ratios at ADF, on the order of the one measured at the source level by Keita et al. (2018). This is also shown by WSOC relative importance which is expected for wood burning following Yu et al. (2018), Tang et al. (2016), Feng (2006) and Saxena and Hildemann (1996) and by the strong correlation of WSOC with biomass burning K^+ tracer.

Chloride is most likely associated with sea salt origin (normal chloride concentrations represent at least 55% of marine aerosols following Goldberg (1963)) or secondary aerosol production (Li et al., 2016). Since chloride relative concentration at the ADF site remains lower than the that of sea-sal aerosols, the secondary production source would be the better explanation for high chloride concentrations observed at ADF. The size distributions of Cl^-, K^+, NH_4^+ and SO_4^{2-} support this conclusion : the predominance of these elements in fine particle mode at the ADF site would be associated with anthropogenic emissions, particularly biomass combustion and domestic fires, or with secondary inorganic aerosols origin. This is confirmed by Cl^-/Na^+ ratio values as shown earlier. Contrarily, Ca^{2+} and NO_3^- contributions to the total ions at the ADF

site peak mainly in the large particle fraction and may be attributed to quasi natural origin, primarily to dust emissions and nitrate formation by reaction processes, respectively. In addition, Na^+ and Mg^{2+} display similar size distributions at the ADF site, with the major contribution in the coarse particle fraction, suggesting the common sea salt origin of these two elements (Belis et al., 2013).

As we have shown above, the lower proportion of metal elements at the ADF site (6.5% of the bulk concentration) can be explained by the less dominant influence of re-suspended dust particles compared to traffic sources. Elements such as Cr, Mn, Pb and Ni have less seasonal variability than other metallic elements. These small proportions of these non-crust elements suggest a low contribution of elements emitted mainly by anthropogenic activities such as industrial processes (Viana et al., 2007 and 2008; Minguillón et al., 2014). Finally, the Zn/Cd ratio has been also examined. A value of 29 close to ratio reported for gasoline vehicle (27, Qin et al., 1997) is obtained for the ADF site, indicating that this site is also impacted by traffic sources.

High values of WSOC/OC ratios are expected to be harmful to health (Ramgolam et al., 2009, Val et al., 2013). This effect is being enhanced by the particulate size measured at this site (Kim et al., 2003; Wilson et al., 2002). Indeed, the relative mass distribution of PM and OC particle sizes shows a major contribution of particles less than 1 µm (as high as 85% of PM). This could be due to the fact that carbonaceous aerosols are formed near emission sources and are mainly of submicron size (Boucher, 2012). Nevertheless, note that EC also presents large coarse particle contribution. This could be due to the importance of wood burning at this site with less efficient combustion and large particle emissions (Watson et al., 2011).

In terms of seasonality, higher concentrations of aerosol mass, OC, WSOC, EC and total water soluble ionic species (SO_4^{2-}, NH_4^+ and NO_3^-) are observed in WS2015 and WS2016 than in DS2016. This may be explained by a more incomplete combustion in the wet seasons than in DS2016 due to the use of moist wood for cooking and smoking fish, which leads to large amount of smoke and higher particulate emission factor values. Note that DS2017 values are as important as the ones of wet seasons, which will be explained later in the text. With regard to WSOC, their variabilities may be also linked to meteorological factors, such as solar radiation (Tang et al., 2016; Favez et al., 2008) and relative humidity (Liang et al., 2016). At ADF site, temperatures are roughly similar in both seasons. However, RH variability may play a role since it is higher in wet season than in dry season. Finally, our results indicate no clear seasonal cycle for Cl^-, which confirms its anthropogenic origin, as previously shown.

576 **4.2. Traffic sites (Abidjan traffic and Cotonou Traffic sites)**

577 Let us recall first that the two traffic sites have been chosen since they are representative of the
578 traffic diversity in West Africa. At CT site, both personal cars, taxis and an important two-
579 wheel fleet may be found whereas at AT site, there are buses, taxis and personal cars. Also, the
580 distance between the site and the traffic sources is the same for the two traffic sites, slightly
581 larger than the distance between the site and the wood burning sources at ADF site.
582 In these two sites, concentrations are high with PM2.5 values well above the WHO guidelines.
583 Average aerosol mass, EC, OC, dust and water soluble ionic concentrations (with NO_3^- and
584 Ca^{2+} maximum at AT and CT sites respectively) are higher at CT than at AT site by a factor of
585 1.5 to 2. Note that this poor air quality found in Cotonou has been reported by Cachon et al.
586 (2014). The higher values found in Cotonou could be due to more intense traffic in Cotonou
587 than in Abidjan. Also in Cotonou, this traffic is associated with the lack of public transportation
588 and the use of highly polluted mopeds (aged over 15 years) (Gounougbe, 1999; Avogbe et al.,
589 2011), despite the effort in the last 10 years to restrict their use. Several studies such as MMEH
590 (2002) have shown that more than 94,000 mopeds and 350,000 second-hand vehicles are in
591 circulation in Cotonou. Other factors contributing to the local pollution include outdoor
592 restaurants using charcoal and motorcycle garages, which are more present around the Cotonou
593 traffic site compared to Abidjan site. It also includes anthropogenic dust. Indeed, at Cotonou,
594 the lack of road infrastructure favours the resuspention of dust particles. Finally, other sources
595 may potentially influence aerosol seasonal composition in these two sites, including marine
596 aerosols, transported dust and biomass burning particles as well as anthropogenic aerosols from
597 the surrounding countries (Figure 5). Note also that source enrichment factor values show that
598 about 17% of trace element concentrations are of anthropogenic origin at both traffic sites and
599 that the relative importance of total carbon in mass is higher at AT than at CT sites.
600 Aerosol mass, composition and size depend on the season and the two traffic sites are differently
601 affected. The EC and OC concentrations measured in both traffic sites and averaged per season
602 are higher in dry than in wet season. Such variations may be explained by several factors:
603 particulate wet deposition occurring during the wet season, reduction of traffic flow due to
604 school vacations and meteorological influence. Higher EC and OC concentrations are obtained
605 at CT than at AT sites in dry seasons whereas no statistical difference may been found between
606 the two sites in wet seasons. Such a result is mainly explained by figures 5. In wet seasons,
607 similar backtrajectory pattern may be observed for both sites whereas in dry seasons, CT traffic
608 site only would be influenced by Nigerian anthropogenic sources.

In terms of WSOC concentrations, concentrations at the AT site are on average higher than those recorded at the CT site in the wet season, but lower in dry season. The presence of dust can produce semi-volatile organic gas scavenging and therefore WSOC and OC enhancement. Such a phenomenon can explain the highest WSOC concentrations observed in dry season at the CT site where dust concentrations are highest (see dust paragraph). Moreover, this can also explain why the maximum WSOC are in coarse particles at CT, while at AT maximum values are in ultra-fine particles.

Total WSI concentrations are larger at AT site in the wet than in the dry season with higher values in coarse particles. At CT site, total WSI concentrations in fine particles are higher in the dry than in the wet season whereas same values are obtained in coarse particles for both seasons. Note that CT values are generally higher than AT values with a more important contribution of fine particles in the dry season. These WSI variations can be explained by the relative importance of Ca^{2+}, SO_4^{2-} and NO_3^- in both sites.

First, Ca^{2+} contribution to total WSI is higher in CT site than in AT site with no clear seasonal variation at CT site and higher values in dry season than in wet season at AT site. Also at CT, fine and coarse Ca^{2+} particles are in the same range, whereas coarse Ca^{2+} particles are predominant at AT site. Such feature may be explained by the impact of dust sources including long-range dust transport at Abidjan and a combination of long-range dust transport and road resuspension at Cotonou.

Second, the relative contribution of SO_4^{2-}, NH_4^+ and NO_3^- as a percentage of total WSI in the different particle modes is reduced in the wet season. During the wet season, the clean winds surrounding the ocean before reaching the measurement sites could contribute to lower the proportion of these species, in addition to the scavenging processes during the rainy days. Unlike the wet season, a relatively good correlation with r^2 of 0.87 (SO_4^{2-} versus NH_4^+), 0.73 (NO_3^- versus NH_4^+) and 0.87 (SO_4^{2-} versus NO_3^-) has been found in coarse particles, indicating similar sources for these three species during the dry season. In order to try to identify these sources, the ratio of SO_4^{2-}/Ca^{2+} and NO_3^-/Ca^{2+} has been determined. The average SO_4^{2-}/Ca^{2+} and NO_3/Ca^{2+} ratios in combined coarse particles (1.07 and 2.58 during the wet season and 0.33 and 1.60 during the dry season) are higher than the corresponding ratios for typical soil (0.026 and 0.003, respectively). On the other hand, the SO_4^{2-}/Ca^{2+} ratio increases in the fine particles (5.07 during the wet season and 2.53 during the dry season), while that of NO_3^-/Ca^{2+} remains almost constant (2.86 during the wet season and 1.65 during the dry season). This implies that the atmosphere at AT and CT sites is enriched by SO_4^{2-} formed as anthropogenic secondary particles, possibly from sulfur containing pollution sources (Seinfield and Pandis, 1998),

particularly in fine particle mode, and by NO_3^- mostly coming from nitrogen containing sources in all particle sizes. The higher contributions of these elements during the dry season could result from a combination of several factors: 1) an atmosphere loaded with dust favoring heterogeneous chemistry to obtain secondary aerosol and the rise of biomass burning emissions; 2) the increase of photochemical activity and higher concentrations of hydroxyl radicals in the dry season, which can oxidize SO_2 from combustion (Arndt et al., 1997) to SO_4^{2-} (Li et al., 2014) ; and 3) the wind transport of anthropogenic secondary particles from the industrial zone located upstream from our sites. Finally, the proportion of Cl^- relative to the total mass of ions is highest for coarse particles at both traffic sites especially during the wet season, suggesting that Cl^- at AT and CT sites if from natural origin and probably from sea salt emissions.

If we focus now on dust during the two wet seasons, concentrations are higher in 2016 than in 2015 at CT and AT sites for coarse particles (no data of fine particles are available in WS2016). This is consistent with observed aerosol optical depth (AOD) values at CT, which increased by a factor of 2 between 2015 and 2016. No AOD value is given by Léon et al. (2019) at Abidjan in WS2015 to allow such comparison in Abidjan. Moreover, during the wet season, an Angström coefficient (AE) on the order of 1 has been found at CT site, indicating smaller particles that could be due to road resuspension. It is interesting to note that during WS2016, AOD and AE are respectively higher and lower at Abidjan than at Cotonou. Again, this is consistent with our dust concentrations at CT site. In Abidjan, we could assume that another source of Ca^{2+}, which is not taken into account in our dust calculations, may explain our dust concentration data. That may be the result of anthropogenic Ca^{2+} emissions from residential combustion, more important in 2016 than in 2015 as shown earlier (http://naei.beis.gov.uk/overview/pollutants?pollutant_id=84).

The relative contribution of dust generally peaks in the coarse mode and, to a lesser extent, in the fine mode, reflecting their natural origin. It is interesting to note that the dust contribution observed in this study for the year 2016 at the Abidjan site is in agreement with the results of Xu et al. (2019) which show a PM2.5 dust contribution of 35-50% compared to our values of 18-52%.

4.3. Abidjan Waste Burning site

Concentrations measured at AWB site are slightly lower than values found in the other sites. This can be explained by the larger distance of the site to the main studied source (here waste burning source) than in the other sites. However, PM2.5 values are also higher than WHO guidelines. +

Aerosol mass, EC and OC concentrations are higher in dry than in wet season, which suggests less waste burning activities during the wet season or impacts of other local anthropogenic sources or long-range biomass burning sources. Highest values are found in DS2017 with the lowest OC/EC ratio, as at AT site. OC/EC ratio is highly variable at AWB (1-10) which confirms that AWB site may be impacted by different types of sources as well as by secondary aerosol organic formation which can be detected for OC/EC higher than 2 (Turpin et al. 1990; Hildermann et al. 1991; Chow et al. 1996). Note that OC/EC typical for waste burning source is of the order of 8 (Keita et al., 2018).

It is also observed that at the AWB site, PM mass concentrations are mainly distributed in C mode (30-44%) over the entire period of study, excepted during the WS2015, and to a lesser extend in F mode (21-44%). EC and OC being mainly distributed in C and UF modes. Water-soluble fraction of organic carbon is important (32%) and on the order of the one found at AT site. Same for WSI concentrations and WSI composition. At AWB, WSI values are globally slightly higher in wet than in dry season. However, it is interesting to underline that Ca^{2+} is much higher in dry season than in wet season, especially in DS2017. This is in agreement with dust concentrations and trace element concentrations, which have been found to be maximum at AWB, reaching 35.8% of the total PM mass in the dry season. These maximum percentages are due to the large contribution of both Al and Na crustal elements which account for about 26%. Also note that Cu/Sb of 0.08 in DS2017, which indicate an influence of re-suspended particles. A Zn/Cd value of 56 is obtained for the AWB site which is in close agreement with values reported for oil burning (Watson et al., 2001, Samara et al., 2003). That could indicate that oil might be one of the waste burning materials.

Our result suggests that AWB aerosol mass is influenced by a mix of sources, including fuel combustion and mineral salt from sources around the measurement site, associated to long-range source impact of dust and biomass burning which will be further discussed in the next paragraph.

4.4. Interannual variability of aerosols in Abidjan and Cotonou

EC and OC concentrations are generally higher in DS2017 than in DS2016 for all the sites. This is not due to the meteorological condition, which is similar in both years. This is also not due to biomass burning impacts. Indeed, when looking at MODIS burnt areas for our period of study (http://www.aeris-data.fr/redirect/MODIS-MCD64A1), burnt areas of west African savannas are higher in 2016 than in 2017. Therefore, carbonaceous aerosol concentrations should be higher in 2016. Then, this could be due to a counter effect between biomass burning emission

711 strength and air mass transport efficiency. As a result, biomass burning impact could not explain
712 the difference in EC and OC during the dry season between 2016 and 2017. Rather, this is due
713 to the variability of local sources. In DS2016 in Abidjan, there was a general strike of civil
714 servants of the State with important consequences on urban activities. Lower activities were
715 observed (lower fish smoking emissions, lower traffic ..) in DS2016 compared to DS2017, thus
716 explaining the lower EC and OC concentrations at Abidjan sites. In Cotonou, highest
717 carbonaceous aerosol values in DS2017 may be explained by backtrajectory patterns: Cotonou
718 would be impacted by air masses coming from the high polluted Lagos (Nigeria) area in that
719 period whereas from less polluted northern areas in DS2016. Such an assumption is validated
720 by the AOD values at 550nm from MODIS satellite images (http://www.aeris-
721 data.fr/redirect/MODIS-MCD64A1), which show very high particulate concentrations in the
722 Guinean Golf (Figure 14).
723 This figure also shows the AOD difference between Cotonou and Abidjan for DS2017, with
724 higher values at Cotonou than in Abidjan for the campaign period, in agreement with our
725 measurements of aerosol mass, EC, OC and dust. This is confirmed by the DACCIWA
726 sunphotometer AOD and Angström coefficient (AE) measurements at Abidjan and Cotonou
727 (Léon et al., 2019; Djossou et al., 2018). Indeed, in DS2017, during our period of
728 measurements, mean AOD in Cotonou is of the order of 1.3 versus 0.9 in Abidjan for an AE of
729 0.6 for both sites, which clearly indicates the presence of coarse dust particles.
730 Finally, aerosol mass and dust concentrations have been seen to be higher in DS2016 than in
731 DS2017 in Abidjan whereas values are on the same order of magnitude at Cotonou. Such high
732 values at Abidjan in DS2016 can be explained by the back-trajectory pattern with air-masses
733 all coming from northern dusty areas in DS2016 (Bodélé depression in Tchad, Prospero et al.
734 (2002), Washington et al., (2003), Knippertz et al. (2011), Balarabe et al., (2016)) and/or from
735 northern dusty countries (Mali, Niger) (Ozer, 2005), whereas in DS2017, contribution of
736 southern marine clean air-masses may also be noted.
737 In the wet season, aerosol mass, EC and OC are higher in WS2015 than in WS2016. This may
738 be due to particulate wet deposition, more efficient in WS2016 which have been seen earlier to
739 be more rainy (4.7mm) than in WS2015 (2mm). Moreover, at AT site, dust concentrations are
740 higher for coarse particles in WS2016 than in WS2015. Such variations may be explained by
741 long-range dust sources and/or road dust resuspension processes. As no dust event has been
742 noticed, local source explanation seems to be more evident.
743 In AT, CT and AWB, OC/EC ratios are globally on the same order for WS2015, WS2016 and
744 DS2016, with values lower than for DS2017. This could be due to lower traffic activities linked

745 to the DS2016 strike and the wet season vacation periods. Indeed, much higher OC/EC ratios
746 measured in DS2017 are typical of those of diesel vehicles (Mmari et al., 2013; Keita et al.,
747 2018). Finally, it is interesting to note that OC/EC ratios measured in this study are in the range
748 of those previously reported for other megacities such as Agra in India with 6.7 (Pachauri et al.,
749 2013), Helsinki in Finland with 2.7 (Viidanoja, 2002), Cairo in Egypt with 2.9 (Favez, 2008),
750 Paris in France with 3.5 (Favez, 2008), and Milan in Italy with 6.6 (Lonati et al., 2007).
751
752 **4.5. Comparison with literature data**
753 Firstly, the comparison between our data and other DACCIWA results including other time
754 sampling focuses on PM2.5 levels, since these particle sizes are relevant for health impact
755 studies (Xing et al., 2016). In addition to our values, Figure 7 presents data from Xu et al. (2019)
756 using personal samplers collected in the same area and at the same dates in 2016 during 12h on
757 women at the ADF site, students at the AWB site and drivers at the CT site, and from Djossou
758 et al. (2018) study based on one week exposed filters collected at the same areas and for the
759 same periods as this study. We note that PM2.5 directly measured on women are 2.3 and 0.9
760 times our values obtained at the ADF site in dry and wet seasons, respectively, and 3.4 and 4.9
761 times higher on students than at the AWB site, and 1.6 and 2.1 times higher on drivers than at
762 the CT site. Also, our values are on average 1.6, 3, 5 and 8 times higher than weekly-integrated
763 values of Djossou et al. (2018) including our 3 days of measurements at the AWB, ADF, AT
764 and CT sites respectively. As it may be seen, the lowest concentrations are observed in Djossou
765 et al. (2018), whereas the highest concentrations are recorded in Xu. et al. (2019). This is valid
766 for all sites, seasons and campaigns. Differences between our values and Djossou values may
767 be explained by the sampling times of the two studies. Indeed, as recalled, Djossou
768 measurements are weekly integrated, taking into account diurnal activities during all the week,
769 including week-end and nights which have expected lower PM2.5 concentrations. Our study
770 includes only maximum pollution conditions for each site. The highest differences occur for
771 the traffic sites. This may be clearly understood since diurnal and weekly variations of traffic
772 sources are the most variable. Comparison between our values and Xu et al. (2019) values is
773 also interesting. Indeed, it is at the ADF site that on-site and women PM2.5 concentrations are
774 the closest, which shows that this site is the most representative of the pollution exposure to
775 women. The biggest differences are found at the AWB site. As already mentioned, distance
776 from the site to the waste burning source is more important than for other sites, which explains
777 why concentrations obtained on students who are leaving close to the sources are much higher
778 than on-site concentrations. At the Cotonou traffic site, measurements taken from people are

779 also higher than on site measurements. Such differences can be explained by additional
780 pollution exposure as people move around. Note that the sampling technique may also play a
781 role in such a comparison. In terms of seasonal variation, our results are in agreement with long-
782 term EC measurements obtained by Djossou et al. (2018) for the same sites and period. Finally,
783 Table 4 compares our mean PM2.5 results obtained from 3-hour sampling for three consecutive
784 days to literature data for different traffic sites in the world given at a daily scale. It is interesting
785 to note that our values are situated at the higher end of the range of PM2.5 data observed from
786 the other sites.
787 Secondly, Table 5 compares our OC and EC values to those obtained by Djossou et al. (2018)
788 and Xu et al. (2019) as previously described for the same period and the same sites. Again, it is
789 interesting to note that Djossou's values are in general lower than ours. Indeed, for the wet and
790 dry seasons, our OC measurements are 4 and 1.4 times higher than Djoussou's at the AT site,
791 2.1 and 5.7 times higher at the CT site, and 2.5 and 2.5 times higher at the ADF site,
792 respectively. As for PM2.5, this can be explained by the different sampling times between our
793 experiments that were performed at the peak of urban activities, while Djossou's dataset
794 represents weekly integrated values. Differences at the ADF site are largely explained by the
795 temporal pattern of fish smoking activities which take place every day, only in the morning, as
796 such the associated pollution is not well represented in the weekly sampling. Finally, there are
797 less differences at the AWB site between both datasets. As above explained, there are no marked
798 temporal variations of concentrations at AWB site. The predominant waste burning emissions
799 impacting our site can occur night and day, week-days and week-end since origin of such
800 burning can be either anthropogenic or from spontaneous combustion. It may be also recalled
801 that another reason of agreement between both datasets may come from the large distance
802 between the site and the local and regional sources. Comparisons made between our values and
803 those of Xu's personal data show that both OC and EC are of the same order at the ADF site,
804 whereas Xu values are higher than ours at the CT and AWB sites. This result is in agreement
805 with what we found with PM2.5 concentrations as detailed above. Finally, Table 6 presents OC
806 and EC for the PM2.5 comparison between our values and other recent studies dealing with
807 traffic sites in other regions of the world and with similar operational conditions. We find that
808 our values are situated in the middle of the range observed in these different studies. Briefly, as
809 presented in Table 7, it is interesting to compare our WSOC concentrations to literature data
810 for different traffic sites of the world. We note that our values are on the same order as values
811 found in Asia and higher than those found in Europe.

Thirdly, the percentages of the total WSI to PM mass (15-20%) at the three Abidjan sites (ADF, AWB and AT) are in the same order of magnitude than the data from PM2.5 personal exposure samples collected at the same locations in 2016 by Xu et al. (2019). Our results also are very close to the ionic contribution of 9% of the PM10 mass found at the urban curbside site in Dar es Salaam in Tanzania during the wet season 2005 by Mkoma (2008).

5. Conclusion

This paper presents the mass and the size-speciated chemical composition of particulate matter (PM) obtained during the dry and wet seasons in 2015, 2016 and 2017. During each campaign, 3-hour sampling at the peak period of pollution for three consecutive days was performed at three sites in Abidjan, representative of domestic fire (ADF), waste burning (AWB) and traffic (AT) sources, and at one traffic site in Cotonou (CT).

It is important to underline that our results and their temporal variations are very sensitive to (1) the source activities whose pollution levels are highly linked to socio-economic status of each city; (2) the impact of imported pollution (sea-salt, biomass burning, dust, anthropogenic emissions from neighboring countries), according to air mass origins; and (3) the particle wet deposition.

The comparison between our results and other DACCIWA measurements underlines the importance of the distance of the chosen site to the sources. At the source level (such as ADF), pollution results at the site are in agreement with exposure of people living at this site. However, at the other sites, comparison is more difficult since the sites are under the influence of a mix of transported sources. That shows the key importance of exposure studies to estimate air quality and health impacts. That shows also the need of long-term studies to really understand role of imported sources in urban air quality.

The main striking feature is that PM2.5 values are well above the annual and daily WHO guidelines of 25 and 10 $\mu g.m^{-3}$, respectively, whatever the site and the season. Also, measured concentrations from this study are situated in the middle to the high part of the range of worldwide urban aerosol concentrations given at a daily scale. In addition, we have stressed the importance of ultra-fine and fine particles in the studied aerosol and of species such as particulate organic matter and water soluble organic carbon, which are well known to be particularly harmful. This is again a warning signal for pollution levels in African capitals if nothing is done to reduce emissions in the future.

Our study constitutes an original database to characterize urban air pollution from specific African combustion sources. The next step will be to cross such an exhaustive aerosol

chemical characterization to biological data in order to evaluate the impact of aerosol size and chemical composition on aerosol inflammatory properties.

Acknowledgements. The research leading to these results has received funding from the European Union 7th Framework Programme (FP7/2007-2013) under Grant Agreement no. 603502 (EU project DACCIWA: Dynamics-aerosol-chemistry-cloud interactions in West Africa). The authors greatly thank all the colleagues and operators who contribute to sampling during the different campaigns.

Author Contributions

J.A. and C.L. conceived and designed the study. J.A., C.L. and E.T.D. contributed to the literature search, data analysis/interpretation and manuscript writing. J.A., C.L., A.B. and E.T.D. contributed to manuscript revision. J.A., C.L., J.F.L, H.C, V.Y., A.A, C.G, C.Z, E.C and S.K. carried out the particulate samples collection and chemical experiments, analyzed the experimental data.

Additional Information

Figure S1 and Appendix A-D accompany this manuscript can be found in SupplementaryInformation.

Competing financial interests

The authors declare no competing financial interests

References

Adon, M., Galy-Lacaux, C., Yoboué, V., Delon, C., Lacaux, J. P., Castera, P., Gardrat, E., Pienaar, J., Al Ourabi, H., Laouali, D., Diop, B., Sigha-Nkamdjou, L., Akpo, A., Tathy, J. P., Lavenu, F. and Mougin, E.: Long term measurements of sulfur dioxide, nitrogen dioxide, ammonia, nitric acid and ozone in Africa using passive samplers, Atmos. Chem. Phys., 10(15), 7467-7487, doi:10.5194/acp-10-7467-2010, 2010.

Alastuey, A., Querol, X., Castillo, S., Escudero, M., Avila, A., Cuevas, E., Torres, C., Romero, P., Exposito, F. and Garcia, O.: Characterisation of TSP and PM2.5 at Izaña and Sta. Cruz de Tenerife (Canary Islands, Spain) during a Saharan Dust Episode (July 2002),

Atmospheric Environment, 39(26), 4715-4728, doi: 10.1016/j.atmosenv.2005.04.018, 2005.

Arditsoglou, A. and Samara, C.: Levels of total suspended particulate matter and major trace elements in Kosovo: a source identification and apportionment study, Chemosphere, 59(5), 669-678, doi: 10.1016/j.chemosphere.2004.10.056, 2005.

Arndt, R. L., Carmichael, G. R., Streets, D. G. and Bhatti, N.: Sulfur dioxide emissions and sectorial contributions to sulfur deposition in Asia, Atmospheric Environment, 31(10), 1553-1572, doi: 10.1016/S1352-2310(96)00236-1, 1997.

Avogbe, P. H., Ayi-Fanou, L., Cachon, B., Chabi, N., Debende, A., Dewaele, D., Aissi, F., Cazier, F. and Sanni, A.: Hematological changes among Beninese motor-bike taxi drivers exposed to benzene by urban air pollution, African Journal of Environmental Science and Technology, 5(7), 464-472, 2011.

Balarabe, M., Abdullah, K. and Nawawi, M.: Seasonal Variations of Aerosol Optical Properties and Identification of Different Aerosol Types Based on AERONET Data over Sub-Sahara West-Africa, ACS, 06(01), 13-28, doi:10.4236/acs.2016.61002, 2016.

Belis, C. A., Karagulian, F., Larsen, B. R. and Hopke, P. K.: Critical review and meta-analysis of ambient particulate matter source apportionment using receptor models in Europe, Atmospheric Environment, 69, 94-108, doi: 10.1016/j.atmosenv.2012.11.009, 2013.

Bisht, D.S., Dumka, U.C., Kaskaoutis, D.G., Pipal, A.S., Srivastava, A. K., Soni, V.K., Attri, S.D., Sateesh, M., Tiwari, S.: Carbonaceous aerosols and pollutants over Delhi urban environment: Temporal evolution, source apportionment and radiative forcing, Science of the Total Environment, 521-522: 431-445, 2015.

Bouhila, Z., Mouzai, M., Azli, T., Nedjar, A., Mazouzi, C., Zergoug, Z., Boukhadra, D., Chegrouche, S. and Lounici, H.: Investigation of aerosol trace element concentrations nearby Algiers for environmental monitoring using instrumental neutron activation analysis, Atmospheric Research, 166, 49-59, doi: 10.1016/j.atmosres.2015.06.013, 2015.

Cachier, H., Brémond, M.-P. and Buat-Ménard, P.: Carbonaceous aerosols from different tropical biomass burning sources, Nature, 340(6232), 371-373, doi:10.1038/340371a0, 1989.

Cachon, B. F., Firmin, S., Verdin, A., Ayi-Fanou, L., Billet, S., Cazier, F., Martin, P. J., Aissi, F., Courcot, D., Sanni, A. and Shirali, P.: Proinflammatory effects and oxidative stress within human bronchial epithelial cells exposed to atmospheric particulate matter (PM2.5 and $PM_{>2.5}$) collected from Cotonou, Benin, Environmental Pollution, 185, 340-351, doi: 10.1016/j.envpol.2013.10.026, 2014.

Cao, J.J., Lee, S.C., Zhang, X.Y., Chow, J.C., An, Z.S., Ho, K.F., Watson, J.G., Fung, K., Wang, Y.Q. and Shen, Z.X.: Characterization of airborne carbonate over a site near Asian dust source regions during spring 2002 and its climatic and environmental significance, J. Geophys. Res., 110(D3), D03203, doi: 10.1029/2004JD005244, 2005.

Cassee, F. R., Héroux, M.-E., Gerlofs-Nijland, M. E. and Kelly, F. J.: Particulate matter beyond mass: recent health evidence on the role of fractions, chemical constituents and sources of emission, Inhalation Toxicology, 25(14), 802–812, doi:10.3109/08958378.2013.850127, 2013.

Celo, V., Dabek-Zlotorzynska, E., Mathieu, D., Okonskaia, I.: Validation of simple microwave-assisted acid digestion method using microvessels for analysis of trace elements in atmospheric PM2.5 in monitoring and fingerprinting studies, The Open Chemical & Biomedical Methods Journal 3., 141-150, 2010.

Cesari, D., Donateo, A., Conte, M., Merico, E., Giangreco, A., Giangreco, F. and Contini, D.: An inter-comparison of PM2.5 at urban and urban background sites: Chemical characterization and source apportionment, Atmospheric Research, 174-175, 106-119, doi: 10.1016/j.atmosres.2016.02.004, 2016.

Cheng, Z., Jiang, J., Chen, C., Gao, J., Wang, S., Watson, J. G., Wang, H., Deng, J., Wang, B., Zhou, M., Chow, J. C., Pitchford, M. L. and Hao, J.: Estimation of Aerosol Mass Scattering Efficiencies under High Mass Loading: Case Study for the Megacity of Shanghai, China, Environ. Sci. Technol., 49(2), 831-838, doi: 10.1021/es504567q, 2015.

Chiapello, I., Bergametti, G., Chatenet, B., Bousquet, P., Dulac, F. and Soares, E. S.: Origins of African dust transported over the northeastern tropical Atlantic, J. Geophys. Res., 102(D12), 13701-13709, doi: 10.1029/97JD00259, 1997.

Chow, J. C., Watson, J. G., Lu, Z., Lowenthal, D. H., Frazier, C. A., Solomon, P. A., Thuillier, R. H. and Magliano, K.: Descriptive analysis of PM2.5 and PM10 at regionally representative locations during SJVAQS/AUSPEX, Atmospheric Environment, 30(12), 2079-2112, doi:10.1016/1352-2310(95)00402-5, 1996.

Colbeck, I., Nasir, Z. A., Ahmad, S. and Ali, Z.: Exposure to PM10, PM2.5, PM1 and Carbon Monoxide on Roads in Lahore, Pakistan, Aerosol Air Qual. Res., 11(6), 689-695, doi:10.4209/aaqr.2010.10.0087, 2011.

Colette, A., Menut, L., Haeffelin, M. and Morille, Y.: Impact of the transport of aerosols from the free troposphere towards the boundary layer on the air quality in the Paris area, Atmospheric Environment, 42(2), 390-402, doi: 10.1016/j.atmosenv.2007.09.044, 2007.

Dieme, D., Cabral-Ndior, M., Garçon, G., Verdin, A., Billet, S., Cazier, F., Courcot, D., Diouf, A. and Shirali, P.: Relationship between physicochemical characterization and toxicity of fine particulate matter (PM2.5) collected in Dakar city (Senegal), Environmental Research, 113, 1-13, doi:10.1016/j.envres.2011.11.009, 2012.

Ding, A., Huang, X. and Fu, C.: Air Pollution and Weather Interaction in East Asia, Oxford Research Encyclopedias-Environmental Sience, doi: 10.1093/acrefore/9780199389414.013. 536, 2017.

Djossou, J., Léon, J.-F., Akpo, A. B., Liousse, C., Yoboué, V., Bedou, M., Bodjrenou, M., Chiron, C., Galy-Lacaux, C., Gardrat, E., Abbey, M., Keita, S., Bahino, J., Touré N'Datchoh, E., Ossohou, M. and Awanou, C. N.: Mass concentration, optical depth and

carbon composition of particulate matter in the major southern West African cities of Cotonou (Benin) and Abidjan (Côte d'Ivoire), Atmos. Chem. Phys., 18(9), 6275-6291, doi:10.5194/acp-18-6275-2018, 2018.

Doumbia, E.H.T., Liousse, C., Galy-Lacaux, C., Ndiaye, S.A., Diop, B., Ouafo, M., et al. Real time black carbon measurements in West and Central Africa urban sites. Atmospheric Environment. 2012;54(0):529-37.

Draxler, R. R., and G. D. Rolph: Evaluation of the Transfer Coefficient Matrix (TCM) approach to model the atmospheric radionuclide air concentrations from Fukushima, J. Geophys. Res., 117, D05107, doi:10.1029/2011JD017205, 2012.

Du, Z., He, K., Cheng, Y., Duan, F., Ma, Y., Liu, J., Zhang, X., Zheng, M. and Weber, R.: A yearlong study of water-soluble organic carbon in Beijing I: Sources and its primary vs. secondary nature, Atmospheric Environment, 92, 514-521, doi:10.1016/j.atmosenv.2014.04. 060, 2014.

Favez, O.: Caractérisation physico-chimique de la pollution particulaire dans des mégapoles contrastées, Thèse de l'Université PARIS.DIDEROT (Paris 7), France, 2008.

Favez, O., Sciare, J., Cachier, H., Alfaro, S. C. and Abdelwahab, M. M.: Significant formation of water-insoluble secondary organic aerosols in semi-arid urban environment, Geophys. Res. Lett., 35(15), L15801, doi:10.1029/2008GL034446, 2008.

Feng, J., Guo, Z., Chan, C. K. and Fang, M.: Properties of organic matter in PM2.5 at Changdao Island, China - A rural site in the transport path of the Asian continental outflow, Atmospheric Environment, 41(9), 1924-1935, doi: 10.1016/j.atmosenv.2006.10.064, 2007.

Feng, J., Hu, M., Chan, C. K., Lau, P. S., Fang, M., He, L. and Tang, X.: A comparative study of the organic matter in PM2.5 from three Chinese megacities in three different climatic zones, Atmospheric Environment, 40(21), 3983-3994, doi: 10.1016/j.atmosenv.2006.02.017, 2006.

Freitas, M.C., Pacheco, A.M.G., Baptista, M.S., Dionísio, I., Vasconcelos, M.T.S.D. and Cabral, J.P.: Response of exposed detached lichens to atmospheric elemental deposition, Proc. ECOpole., 1(1/2), 15-21, 2007.

Gaga, E. O., Arı, A., Akyol, N., Üzmez, Ö. Ö., Kara, M., Chow, J. C., Watson, J. G., Özel, E., Döğeroğlu, T. and Odabasi, M.: Determination of real-world emission factors of trace metals, EC, OC, BTEX, and semivolatile organic compounds (PAHs, PCBs and PCNs) in a rural tunnel in Bilecik, Turkey, Science of The Total Environment, 643, 1285-1296, doi: 10.1016/j.scitotenv.2018.06.227, 2018.

Gao, Y., Nelson, E. D., Field, M. P., Ding, Q., Li, H., Sherrell, R. M., Gigliotti, C. L., Van Ry, D. A., Glenn, T. R. and Eisenreich, S. J.: Characterization of atmospheric trace elements on PM2.5 particulate matter over the New York–New Jersey harbor estuary, Atmospheric Environment, 36(6), 1077–1086, doi:10.1016/S1352-2310(01)00381-8, 2002.

994 Genga, A., Ielpo, P., Siciliano, T. and Siciliano, M.: Carbonaceous particles and aerosol mass
995 closure in PM2.5 collected in a port city, Atmospheric Research, 183, 245-254, doi:
996 10.1016/j.atmosres.2016.08.022, 2017.

997 Gounougbe, F.: Pollution atmosphérique par les gaz d'échappement et état de santé des
998 conducteurs de taxi-moto (Zemidjan) de Cotonou (Bénin), Thèse de doctorat en Médecine
999 (832), 1999.

1000 Guinot, B., Cachier, H. and Oikonomou, K.: Geochemical perspectives from a new aerosol
1001 chemical mass closure, Atmos. Chem. Phys., 7(6), 1657-1670, doi: 10.5194/acp-7-1657-
1002 2007, 2007.

1003 Guttikunda, S. K. and Calori, G.: A GIS based emissions inventory at 1 km × 1 km spatial
1004 resolution for air pollution analysis in Delhi, India, Atmospheric Environment, 67, 101-
1005 111, doi:10.1016/j.atmosenv.2012.10.040, 2013.

1006 Hara, K., Osada, K., Kido, M., Hayashi, M., Matsunaga, K., Iwasaka, Y., Yamanouchi, T.,
1007 Hashida, G. and Fukatsu, T.: Chemistry of sea-salt particles and inorganic halogen species
1008 in Antarctic regions: Compositional differences between coastal and inland stations, J.
1009 Geophys. Res., 109, D20208, doi:10.1029/2004JD004713, 2004.

1010 He, K., Yang, F., Ma, Y., Zhang, Q., Yao, X., Chan, C. K., Cadle, S., Chan, T. and Mulawa, P.:
1011 The characteristics of PM2.5 in Beijing, China, Atmospheric Environment, 35(29), 4959-
1012 4970, doi: 10.1016/S1352-2310(01)00301-6, 2001.

1013 Hildemann, L. M., Markowski, G. R. and Cass, G. R.: Chemical composition of emissions from
1014 urban sources of fine organic aerosol, Environ. Sci. Technol., 25(4), 744-759, doi:
1015 10.1021/es00016a021, 1991.

1016 Huang, H., Ho, K. F., Lee, S. C., Tsang, P. K., Ho, S. S. H., Zou, C. W., Zou, S. C., Cao, J. J.
1017 and Xu, H. M.: Characteristics of carbonaceous aerosol in PM2.5: Pearl Delta River
1018 Region, China, Atmospheric Research, 104-105, 227-236, doi:
1019 10.1016/j.atmosres.2011.10.016, 2012.

1020 Jaffrezo, J.-L., Aymoz, G., Delaval, C., and Cozic, J.: Seasonal variations of the Water Soluble
1021 Organic Carbon mass fraction of aerosol in two valleys of the French Alps, Atmos. Chem.
1022 Phys., 5, 2809-2821, 2005.

1023 Keita, S., Liousse, C., Yoboué, V., Dominutti, P., Guinot, B., Assamoi, E.-M., Borbon, A.,
1024 Haslett, S. L., Bouvier, L., Colomb, A., Coe, H., Akpo, A., Adon, J., Bahino, J., Doumbia,
1025 M., Djossou, J., Galy-Lacaux, C., Gardrat, E., Gnamien, S., Léon, J. F., Ossohou, M.,
1026 N'Datchoh, E. T. and Roblou, L.: Particle and VOC emission factor
1027 measurements for anthropogenic sources in West Africa, Atmos. Chem. Phys., 18(10),
1028 7691-7708, doi:10.5194/acp-18-7691-2018, 2018.

1029 Khan, Md. F., Shirasuna, Y., Hirano, K. and Masunaga, S.: Characterization of PM2.5, PM2.5-
1030 10 and PM>10 in ambient air, Yokohama, Japan, Atmospheric Research, 96(1), 159-172,
1031 doi:10.1016/j.atmosres.2009.12.009, 2010.

Kim, H., Liu, X., Kobayashi, T., Kohyama, T., Wen, F.-Q., Romberger, D. J., Conner, H., Gilmour, P. S., Donaldson, K., MacNee, W. and Rennard, S. I.: Ultrafine Carbon Black Particles Inhibit Human Lung Fibroblast-Mediated Collagen Gel Contraction, Am J Respir. Cell. Mol. Biol., 28(1), 111-121, doi:10.1165/rcmb.4796, 2003.

Knippertz, P., Tesche, M., Heinold, B., Kandler, K., Toledano, C. and Esselborn, M.: Dust mobilization and aerosol transport from West Africa to Cape Verde - a meteorological overview of SAMUM-2, Tellus B: Chemical and Physical Meteorology, 63(4), 430-447, doi:10.1111/j.1600-0889.2011. 00544.x, 2011.

Kouassi, K. S., Billet, S., GarÃ§on, G., Verdin, A., Diouf, A., Cazier, F., Djaman, J., Courcot, D. and Shirali, P.: Oxidative damage induced in A549 cells by physically and chemically characterized air particulate matter ($PM_{2.5}$) collected in Abidjan, Côte d'Ivoire, J. Appl. Toxicol., doi:10.1002/jat.1496, 2009.

Lamaison, L. : Caractérisation des particules atmosphériques et identification de leurs sources dans une atmosphère urbaine sous influence industrielle, Thèse Doctorat, Univ des Sciences et Technologies, Lille, 2006.

Léon, J.F., Akpo, A., Bedou, M., Djossou, J., Bodjrenou, M., Yoboué, V., et Liousse, C.: Profondeur optique des aérosols sur le sud de l'Afrique de l'Ouest, soumis à ACPD, 2019.

Li, T.-C., Yuan, C.-S., Hung, C.-H., Lin, H.-Y., Huang, H.-C. and Lee, C.-L.: Chemical Characteristics of Marine Fine Aerosols over Sea and at Offshore Islands during Three Cruise Sampling Campaigns in the Taiwan Strait-Sea Salts and Anthropogenic Particles, Atmos. Chem. Phys. Discuss., 1-27, doi:10.5194/acp-2016-384, 2016.

Li, Y., Schwandner, F. M., Sewell, H. J., Zivkovich, A., Tigges, M., Raja, S., Holcomb, S., Molenar, J. V., Sherman, L., Archuleta, C., Lee, T. and Collett, J. L.: Observations of ammonia, nitric acid and fine particles in a rural gas production region, Atmospheric Environment, 83, 80-89, doi:10.1016/j.atmosenv.2013.10.007, 2014.

Liang, L., Engling, G., Du, Z., Cheng, Y., Duan, F., Liu, X. and He, K.: Seasonal variations and source estimation of saccharides in atmospheric particulate matter in Beijing, China, Chemosphere, 150, 365-377, 2016.

Liousse, C., Assamoi, E., Criqui, P., Granier, C., Rosset, R.: Explosive growth in African combustion emissions from 2005 to 2030, Environ. Res. Lett., 9, 035003, 2014.

Lonati, G., Ozgen, S. and Giugliano, M.: Primary and secondary carbonaceous species in $PM_{2.5}$ samples in Milan (Italy), Atmospheric Environment, 41(22), 4599-4610, doi:10.1016/j.atmosenv.2007.03.046, 2007.

Lowenthal, D., Zielinska, B., Samburova, V., Collins, D., Taylor, N. and Kumar, N.: Evaluation of assumptions for estimating chemical light extinction at U.S. national parks, Journal of the Air & Waste Management Association, 65(3), 249-260, doi:10.1080/10962247.2014.986307, 2015.

Mason, B., Moore, B.C.: Principles of Geochemistry, fourth ed. John Wiley and Sons, New York, pp. 46-47, 1982.

Minguillón, M. C., Cirach, M., Hoek, G., Brunekreef, B., Tsai, M., de Hoogh, K., Jedynska, A., Kooter, I. M., Nieuwenhuijsen, M. and Querol, X.: Spatial variability of trace elements and sources for improved exposure assessment in Barcelona, Atmospheric Environment, 89, 268-281, doi: 10.1016/j.atmosenv.2014.02.047, 2014.

Mkoma, S. L.: Physico-Chemical characterisation of atmospheric aerosols in Tanzania, with emphasis on the carbonaceous aerosol components and on chemical mass closure, PhD, Ghent University, Ghent, Belguim, 2008.

Mmari, A. G., Potgieter-Vermaak, S. S., Bencs, L., McCrindle, R. I. and Van Grieken, R.: Elemental and ionic components of atmospheric aerosols and associated gaseous pollutants in and near Dar es Salaam, Tanzania, Atmospheric Environment, 77, 51-61, doi: 10.1016/j.atmosenv.2013.04.061, 2013.

MMEH (Ministère des Mines de l'Energie et d'Hydraulique): Tableau de bord de l'Energie 2002 au Bénin, Direction Générale de l'Energie, 2002.

Ngo, N. S., Asseko, S. V. J., Ebanega, M. O., Allo'o Allo'o, S. M. and Hystad, P.: The relationship among PM2.5, traffic emissions, and socioeconomic status: Evidence from Gabon using low-cost, portable air quality monitors, Transportation Research Part D: Transport and Environment, 68, 2-9, doi: 10.1016/j.trd.2018.01.029, 2019.

Ozer, P.: Estimation de la pollution particulaire naturelle de l'air en 2003 à Niamey (Niger) à partir de données de visibilité horizontale, 2005.

Pachauri, T., Singla, V., Satsangi, A., Lakhani, A. and Kumari, K. M.: Characterization of carbonaceous aerosols with special reference to episodic events at Agra, India, Atmospheric Research, 128, 98-110, doi: 10.1016/j.atmosres.2013.03.010, 2013.

Park, J. H., Mudunkotuwa, I. A., Mines, L. W. D., Anthony, T. R., Grassian, V. H. and Peters, T. M.: A Granular Bed for Use in a Nanoparticle Respiratory Deposition Sampler, Aerosol Science and Technology, 49(3), 179-187, doi:10.1080/02786826.2015.1013521, 2015.

Person, A. and Tymen, G.: Mesurage des particules en suspension dans l'air en relation avec la santé. Pollution atmosphèrique, 271-285, 2005.

Pipal, A. S., Jan, R., Satsangi, P. G., Tiwari, S. and Taneja, A.: Study of Surface Morphology, Elemental Composition and Origin of Atmospheric Aerosols (PM2.5 and PM10) over Agra, India, Aerosol Air Qual. Res., 14(6), 1685-1700, doi:10.4209/aaqr.2014.01.0017, 2014.

Pipal, A. S., Singh, S. and Satsangi, G. P.: Study on bulk to single particle analysis of atmospheric aerosols at urban region, Urban Climate, 27, 243-258, doi: 10.1016/j.uclim.2018.12.008, 2019.

Prospero, J.M., Ginoux, P., Torres, O., Nicholson, S.E., Gill, T.E.: Environmental characterization of global sources of atmospheric soil dust identified with the NIMBUS 7

Total Ozone Mapping Spectrometer (TOMS) absorbing aerosol product, Rev. Geophys., 40, 2-1-31, 2002.

Qin, Y., Chan, C. K. and Chan, L. Y.: Characteristics of chemical compositions of atmospheric aerosols in Hong Kong: spatial and seasonal distributions, Science of The Total Environment, 206(1), 25-37, doi: 10.1016/S0048-9697(97)00214-3, 1997.

Ramgolam K, Favez O, Cachier H, Gaudichet A, Marano F, Martinon L, Baeza-Squiban A: Size-partitioning of an urban aerosol to identify particle determinants involved in the proinflammatory response induced in airway epithelial cells. Part Fibre Toxicol 2009, 6: 10. 10.1186/1743-8977-6-10.

Rengarajan, R., Sudheer, A. K. and Sarin, M. M.: Aerosol acidity and secondary organic aerosol formation during wintertime over urban environment in western India, Atmospheric Environment, 45(11), 1940-1945, doi: 10.1016/j.atmosenv.2011.01.026, 2011.

Samara, C., Kouimtzis, T., Tsitouridou, R., Kanias, G. and Simeonov, V.: Chemical mass balance source apportionment of PM10 in an industrialized urban area of Northern Greece, Atmospheric Environment, 37(1), 41-54, doi:10.1016/S1352-2310(02)00772-0, 2003.

Satsangi, A., Pachauri, T., Singla, V., Lakhani, A. and Kumari, K. M.: Organic and elemental carbon aerosols at a suburban site, Atmospheric Research, 113, 13-21, doi: 10.1016/j.atmosres.2012.04.012, 2012.

Saxena, P., and Hildemann, L.M.: Water-soluble organics in atmospheric particles: a critical review of the literature and application of thermodynamics to identify candidate compounds, J. Atmos. Chem., 24(1), 57-109, 1996.

Sciare, J., Oikonomou, K., Cachier, H., Mihalopoulos, N., Andreae, M. O., Maenhaut, W. and Sarda-Estève, R.: Aerosol mass closure and reconstruction of the light scattering coefficient over the Eastern Mediterranean Sea during the MINOS campaign, Atmos. Chem. Phys., 5(8), 2253-2265, doi:10.5194/acp-5-2253-2005, 2005.

Seinfeld, J. H. and Pandis, S. N.: Atmospheric Chemistry and Physics: from Air Pollution to Climate Change, John Wiley and Sons, Inc. New York, 1998.

Shahsavani, A., Naddafi, K., Jaafarzadeh Haghighifard, N., Mesdaghinia, A., Yunesian, M., Nabizadeh, R., Arhami, M., Yarahmadi, M., Sowlat, M. H., Ghani, M., Jonidi Jafari, A., Alimohamadi, M., Motevalian, S. A. and Soleimani, Z.: Characterization of ionic composition of TSP and PM10 during the Middle Eastern Dust (MED) storms in Ahvaz, Iran, Environ Monit Assess, 184(11), 6683-6692, doi:10.1007/s10661-011-2451-6, 2012.

Stone, R. S., Herber, A., Vitale, V., Mazzola, M., Lupi, A., Schnell, R. C., Dutton, E. G., Liu, P. S. K., Li, S.-M., Dethloff, K., Lampert, A., Ritter, C., Stock, M., Neuber, R. and Maturilli, M.: A three-dimensional characterization of Arctic aerosols from airborne Sun photometer observations: PAM-ARCMIP, April 2009, J. Geophys. Res., 115(D13), D13203, doi: 10.1029/2009JD013605, 2010.

Sullivan, A. P., Weber, R. J., Clements, A. L., Turner, J. R., Bae, M. S. and Schauer, J. J.: A method for on-line measurement of water-soluble organic carbon in ambient aerosol particles: Results from an urban site: on-line measurement of WSOC in aerosols, Geophys. Res. Lett., 31(13), doi: 10.1029/2004GL019681, 2004.

Sun, Y., Zhuang, G., Wang, Y., Han, L., Guo, J., Dan, M., Zhang, W., Wang, Z. and Hao, Z.: The airborne particulate pollution in Beijing - concentration, composition, distribution and sources, Atmospheric Environment, 38(35), 5991-6004, doi: 10.1016/j.atmosenv.2004.07.009, 2004.

Tang, X., Zhang, X., Ci, Z., Guo, J. and Wang, J.: Speciation of the major inorganic salts in atmospheric aerosols of Beijing, China: Measurements and comparison with model, Atmospheric Environment, 133, 123-134, doi: 10.1016/j.atmosenv.2016.03.013, 2016.

Tapsoba, D. : Caractérisation événementielle des régimes pluviométriques ouestafricains et de leur récent changement, Thèse de Doctorat, Univ.Paris-XI (Orsay). 100p, 1997.

Taylor, S. R.: Abundance of chemical elements in the continental crust: a new table, Geochimica et Cosmochimica Acta, 28(8), 1273-1285, doi: 10.1016/0016-7037(64)90129-2, 1964.

Terzi, E., Argyropoulos, G., Bougatioti, A., Mihalopoulos, N., Nikolaou, K. and Samara, C.: Chemical composition and mass closure of ambient PM10 at urban sites, Atmospheric Environment, 44(18), 2231-2239, doi: 10.1016/j.atmosenv.2010.02.019, 2010.

Tunno, B., Longley, I., Somervell, E., Edwards, S., Olivares, G., Gray, S., Cambal, L., Chubb, L., Roper, C., Coulson, G. and Clougherty, J. E.: Separating spatial patterns in pollution attributable to woodsmoke and other sources, during daytime and nighttime hours, in Christchurch, New Zealand, Environmental Research, 171, 228-238, doi: 10.1016/j.envres.2019.01.033, 2019.

Turpin, B. J., Cary, R. A. and Huntzicker, J. J.: An In Situ, Time-Resolved Analyzer for Aerosol Organic and Elemental Carbon, Aerosol Science and Technology, 12(1), 161-171, doi:10.1080/02786829008959336, 1990.

United Nations, Department of Economic and Social Affairs, Population Division (2019). World Population Prospects 2019: Volume II: Demographic Profiles. Made available under a Creative Commons license. http://creativecommons.org/licenses/by/3.0/igo/ 2019

Val, S., Liousse, C., Doumbia, E. H. T., Galy-Lacaux, C., Cachier, H., Marchand, N., Badel, A., Gardrat, E., Sylvestre, A. and Baeza-Squiban, A.: Physico-chemical characterization of African urban aerosols (Bamako in Mali and Dakar in Senegal) and their toxic effects in human bronchial epithelial cells: description of a worrying situation, Part Fibre Toxicol, 10(1), 10, doi:10.1186/1743-8977-10-10, 2013.

Viana, M., López, J. M., Querol, X., Alastuey, A., García-Gacio, D., Blanco-Heras, G., López-Mahía, P., Piñeiro-Iglesias, M., Sanz, M. J., Sanz, F., Chi, X. and Maenhaut, W.: Tracers and impact of open burning of rice straw residues on PM in Eastern Spain, Atmospheric Environment, 42(8), 1941-1957, doi: 10.1016/j.atmosenv.2007.11.012, 2008.

Viana, M., Maenhaut, W., ten Brink, H. M., Chi, X., Weijers, E., Querol, X., Alastuey, A., Mikuška, P. and Večeřa, Z.: Comparative analysis of organic and elemental carbon concentrations in carbonaceous aerosols in three European cities, Atmospheric Environment, 41(28), 5972-5983, doi: 10.1016/j.atmosenv.2007.03.035, 2007.

Viidanoja, J., Sillanpää, M., Laakia, J., Kerminen, V.-M., Hillamo, R., Aarnio, P. and Koskentalo, T.: Organic and black carbon in PM2.5 and PM10: 1 year of data from an urban site in Helsinki, Finland, Atmospheric Environment, 36(19), 3183-3193, doi: 10.1016/S1352-2310(02)00205-4, 2002.

Wang, X., Bi, X., Sheng, G. and Fu, J.: Chemical Composition and Sources of PM10 and PM2.5 Aerosols in Guangzhou, China, Environ Monit Assess, 119(1-3), 425-439, doi: 10.1007/s10661-005-9034-3, 2006.

Washington, R., Todd, M., Middleton, N. J. and Goudie, A. S.: Dust-Storm Source Areas Determined by the Total Ozone Monitoring Spectrometer and Surface Observations, Annals of the Association of American Geographers, 93(2), 297-313, doi:10.1111/1467-8306.9302003, 2003.

Watson, J. G. and Chow, J. C.: Estimating middle-, neighborhood-, and urban-scale contributions to elemental carbon in Mexico City with a rapid response aethalometer, J. Air Waste Manag. Assoc., 51(11), 1522-1528, 2001.

Watson, J. G., Chow, J. C. and Houck, J. E.: PM2.5 chemical source profiles for vehicle exhaust, vegetative burning, geological material, and coal burning in Northwestern Colorado during 1995, Chemosphere, 43(8), 1141-1151, doi:10.1016/S0045-6535(00)00171-5, 2001.

WHO (World Health Organization), 7 million premature deaths annually linked to air pollution. Media Centre news release. Geneva: World Health Organization. (http: //www.who.int/ mediacentre/news/releases/2014/airpollution/en/, 2014.

Wilson, M. R., Lightbody, J. H., Donaldson, K., Sales, J. and Stone, V.: Interactions between ultrafine particles and transition metals in vivo and in vitro, Toxicol. Appl. Pharmacol., 184(3), 172-179, 2002.

Xiang, P., Zhou, X., Duan, J., Tan, J., He, K., Yuan, C., Ma, Y. and Zhang, Y.: Chemical characteristics of water-soluble organic compounds (WSOC) in PM2.5 in Beijing, China: 2011-2012, Atmospheric Research, 183, 104-112, doi: 10.1016/j.atmosres.2016.08.020, 2017.

Xie, Y., Wang, Y., Bilal, M. and Dong, W.: Mapping daily PM2.5 at 500 m resolution over Beijing with improved hazy day performance, Science of The Total Environment, 659, 410-418, doi: 10.1016/j.scitotenv.2018.12.365, 2019.

Xu, H., Léon, J.-F., Liousse, C., Guinot, B., Yoboué, V., Akpo, A. B., Adon, J., Ho, K. F., Ho, S. S. H., Li, L., Gardrat, E., Shen, Z. and Cao, J.: Personal exposure to PM2.5 emitted from typical anthropogenic sources in Southern West Africa (SWA): Chemical characteristics and associated health risks, Atmos. Chem. Phys. Discuss., 1-68, doi:10.5194/acp-2018-1060, 2019.

Xu, J., Zhang, Y., Zheng, S. and He, Y.: Aerosol effects on ozone concentrations in Beijing: a model sensitivity study, J Environ Sci (China), 24(4), 645-656, 2012.

Yu, P., Froyd, K. D., Portmann, R. W., Toon, O. B., Freitas, S. R., Bardeen, C. G., Katich, J. M., Schwarz, J. P., Williamson, C., Kupc, A., Brock, C., Liu, S., Gao, R.-S., Schill, G., Fan, T., Rosenlof, K. H., and Murphy, D. M.: An improved treatment of aerosol convective transport and removal in a chemistry-climate model, Geophys. Res. Lett., submitted, 2018.

Zghaid, M., Noack, Y., Bounakla, M., and Benyaich, F.: Pollution atmosphérique particulaire dans la ville de Kenitra (Maroc), Pollution atmosphérique [En ligne], N° 203, mis à jour le 12/10/2015,URL:http://lodel.irevues.inist.fr/pollution-atmospherique/index.php?id=1184, https://doi.org/10.4267/pollution-atmospherique.1184

Zhang, X. Y., Gong, S. L., Shen, Z. X., Mei, F. M., Xi, X. X., Liu, L.C., Zhou, Z. J., Wang, D., Wang, Y. Q., and Cheng, Y.: Characterization of soil dust aerosol in China and its transport and distribution during 2001 ACE-Asia: 1. Network observations, J. Geophys. Res. Atmos., 108(D9), 4261, doi:10.1029/2002JD002632, 2003.

Figure caption

Figure 1: Map of the city of Abidjan reporting the geographical location of DACCIWA urban sampling sites.

1254 Figure 2: Map of the city of Cotonou reporting the geographical location of DACCIWA urban
1255 sampling site.

1256 Figure 3: Pictures of the different sampling sites: (a) Traffic in Cotonou (Benin, CT station),
1257 (b) Waste burning in Abidjan (Côte d'Ivoire, AWB station), (c), Domestic fire, showing
1258 smoking activity in Yopougon, Abidjan (Côte d'Ivoire, ADF station), (d) " woro-woro
1259 and Gbaka " traffic in Abidjan (Côte d'Ivoire, AT station).

1260 Figure 4: Wind, pressure and temperature diagram at Abidjan and Cotonou during the different
1261 campaigns.

1262 Figure 5: Back trajectories arriving at Abidjan (a) and Cotonou (b) for each season (WS2015,
1263 WS2016, DS2016 and DS2017).

1264 Figure 6: Aerosol Mass concentrations at the different study sites for each campaign and for the
1265 different sizes (C in black, Fine in light Grey, Ultra-fine in grey). Bulk aerosol mass is
1266 indicated in boxes.

1267 Figure 7: Comparison of PM2.5 mass concentrations in $\mu g.m^{-3}$ at the four sites with those
1268 obtained by Djossou et al. (2018) and Xu et al. (2019) for the same sites and periods.
1269 Data for the following weeks were then selected in Djossou et al. (2018): 20-27/07/2015
1270 for WS15, 4-11/01/2016 for DS16, 4-11/07/2016 for WS16 and 9-16/01/2017 for DS17.

1271 Figure 8: EC relative concentrations in each size classes (C in black, Fine in light grey, Ultra-
1272 fine in grey) at the different study sites for each campaign. Bulk EC concentration for
1273 each site is indicated in boxes.

1274 Figure 9: OC relative concentrations in each size classes (C in black, Fine in light grey, Ultra-
1275 fine in grey) at the different study sites for each campaign. Bulk OC concentration for
1276 each site is indicated in boxes.

1277 Figure 10: OC/ EC ratio for the different campaigns and sites for each aerosol size (C in black,
1278 Fine in light grey, Ultra-fine in grey). Each box shows the median and the first and the
1279 third quartiles.

1280 Figure 11: Water-soluble ionic species speciation for each site, each campaign and each aerosol
1281 size.

1282 Figure 12: Dust concentrations at the different study sites for each campaign and for the
1283 different sizes (C in black, Fine in light grey, Ultra-fine in grey).

Figure 13: Size-speciated aerosol chemical composition for each site, for each campaign and each aerosol size.

Figure 14: MODIS Aerosol optical depth regional distribution over West Africa. Data are for 2017, focusing on our campaign date at Abidjan (a-c 01/11-12-left part) and Cotonou (b-d 01/6-7, right part).

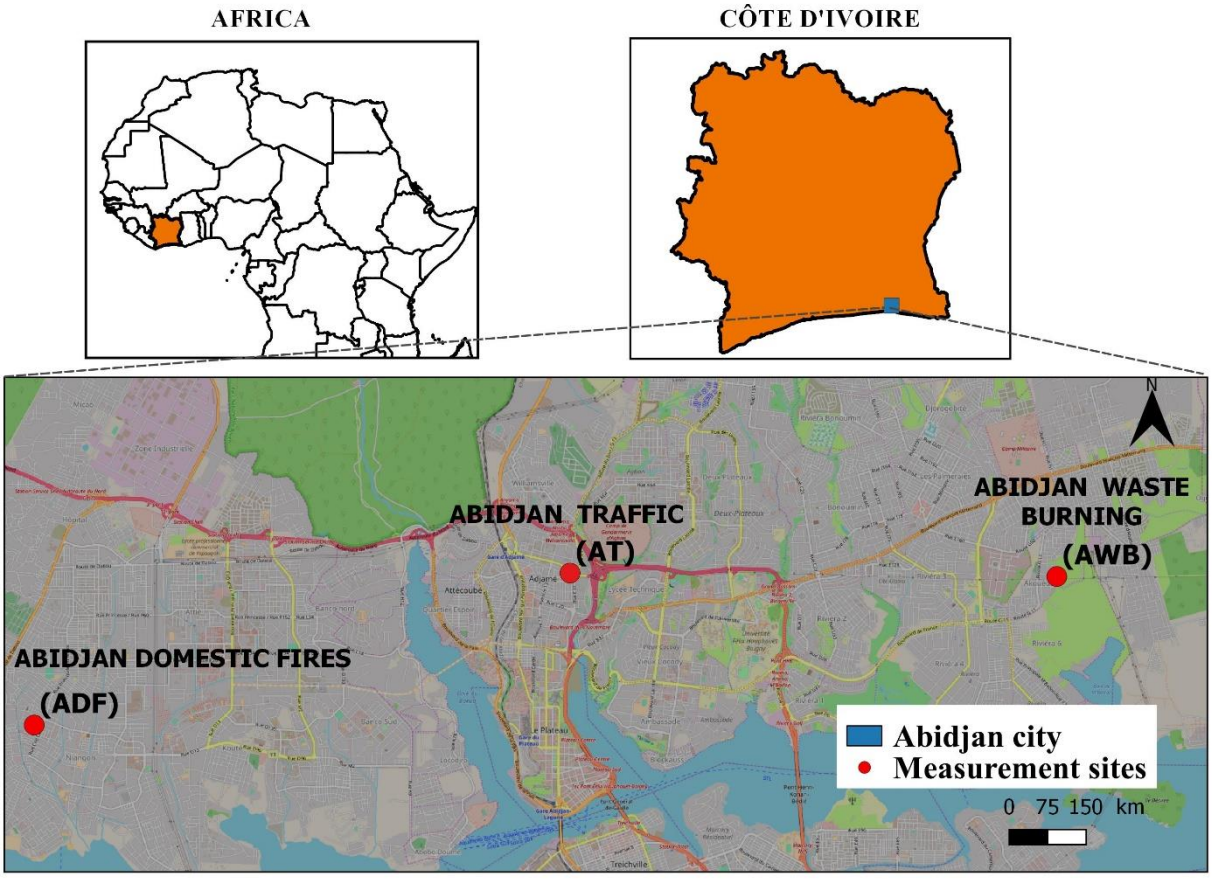

Figure1

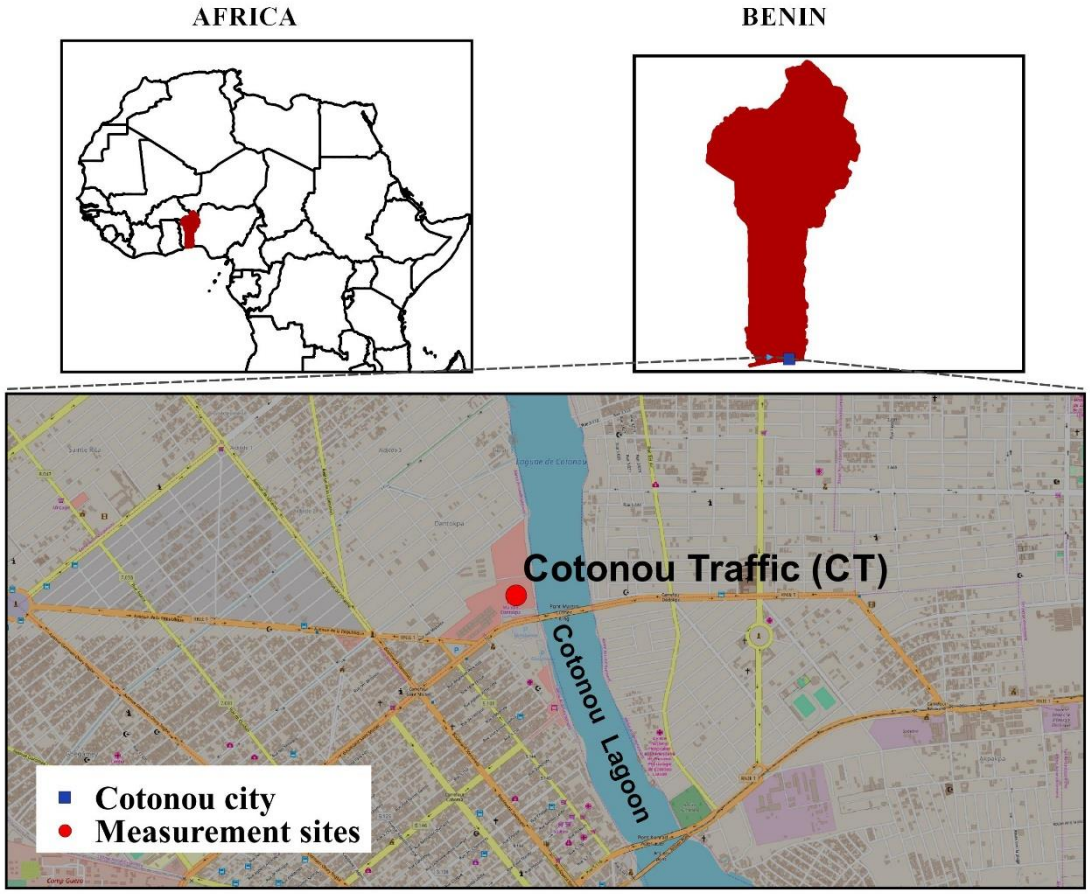

Figure 2

Figure 3

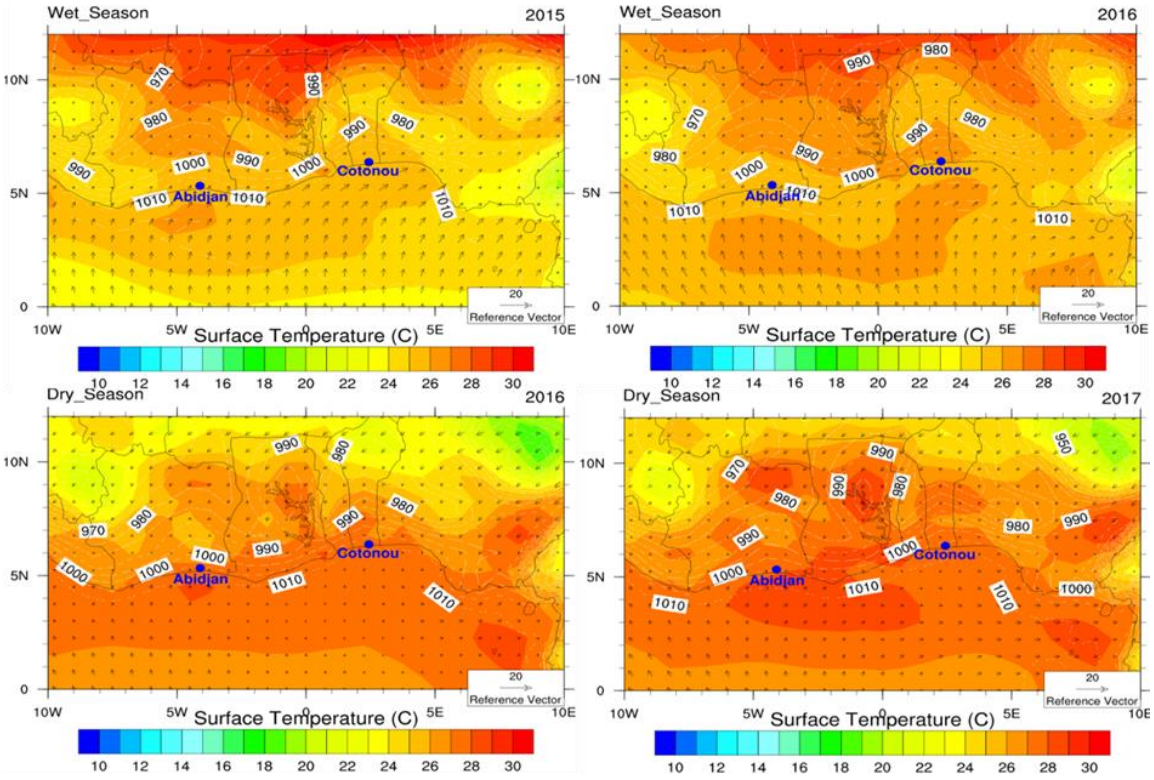
Wet_Season
2015
Wet_Season
2016
Dry_Season
2016
Dry_Season
2017
Abidjan
Cotonou
Reference Vector
Surface Temperature (C)
10N
5N
0
10W
5W
0
5E
10E
10 12 14 16 18 20 22 24 26 28 30

Figure 4

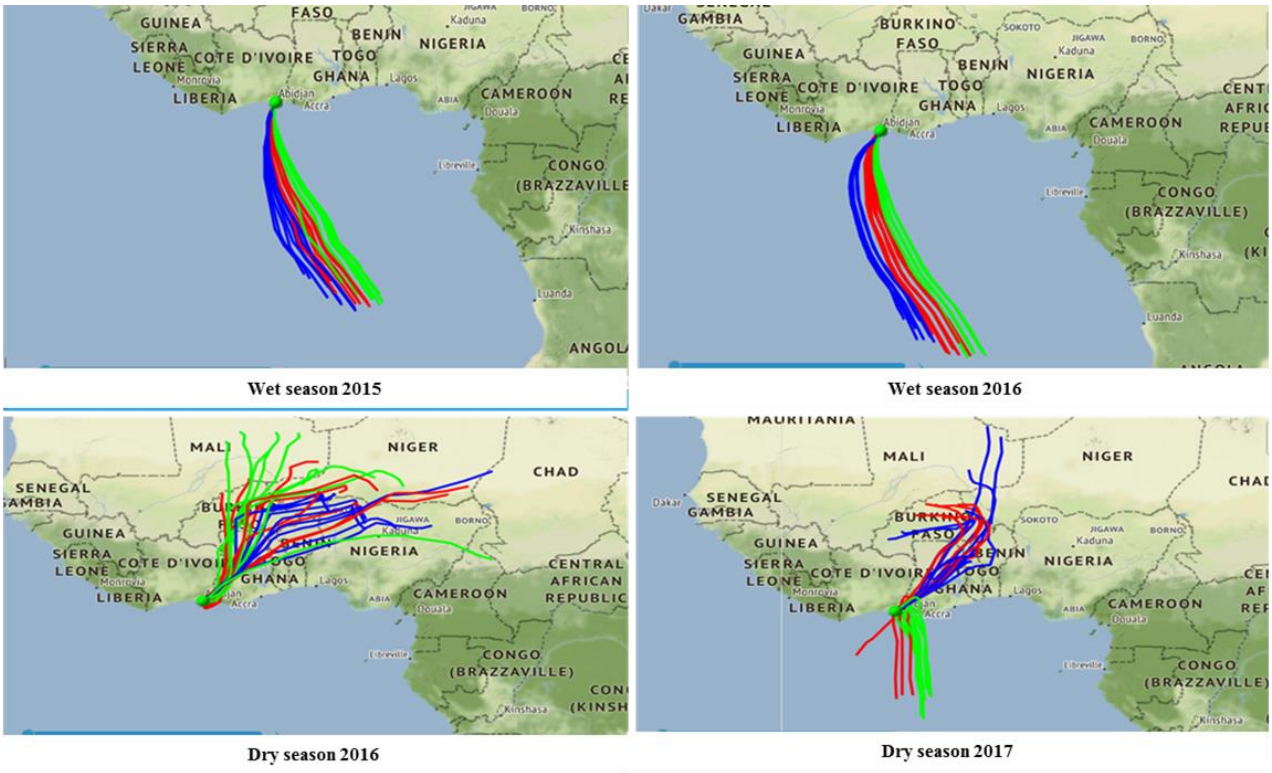

Figure 5-a

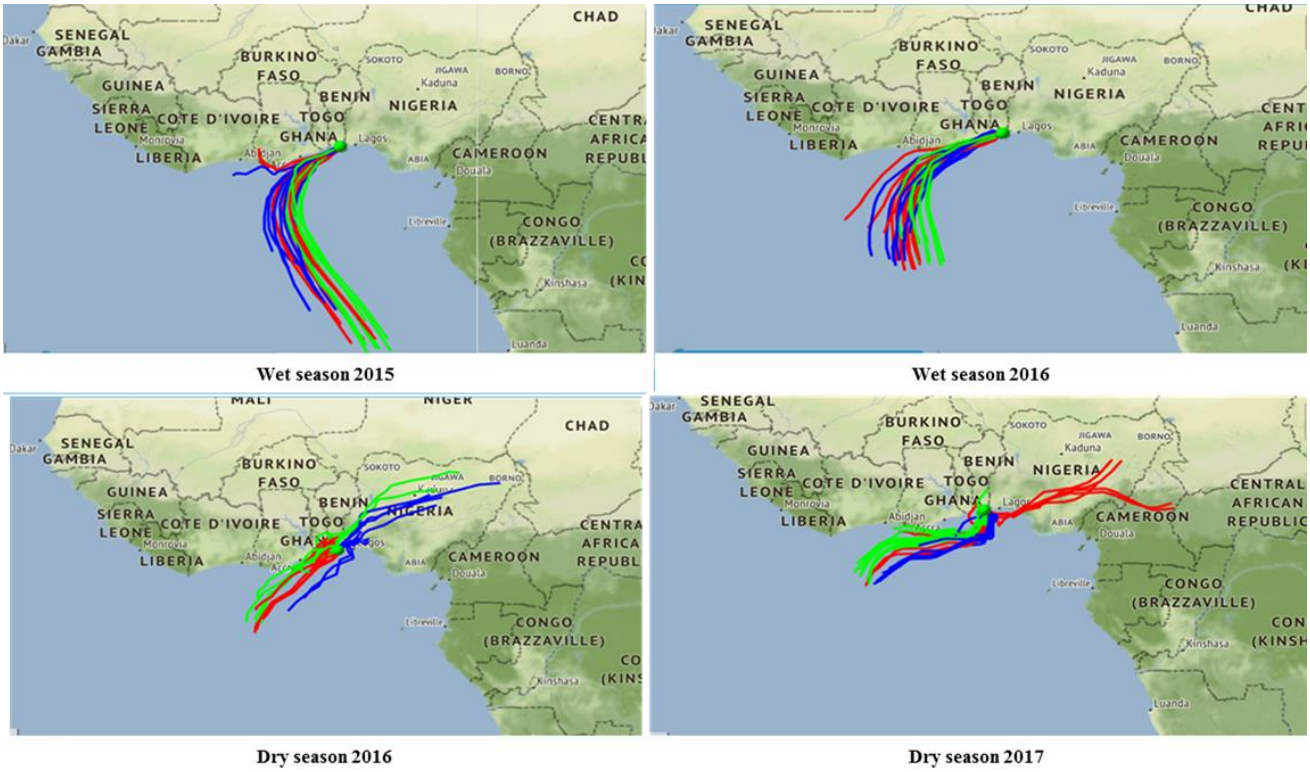

Figure 5-b

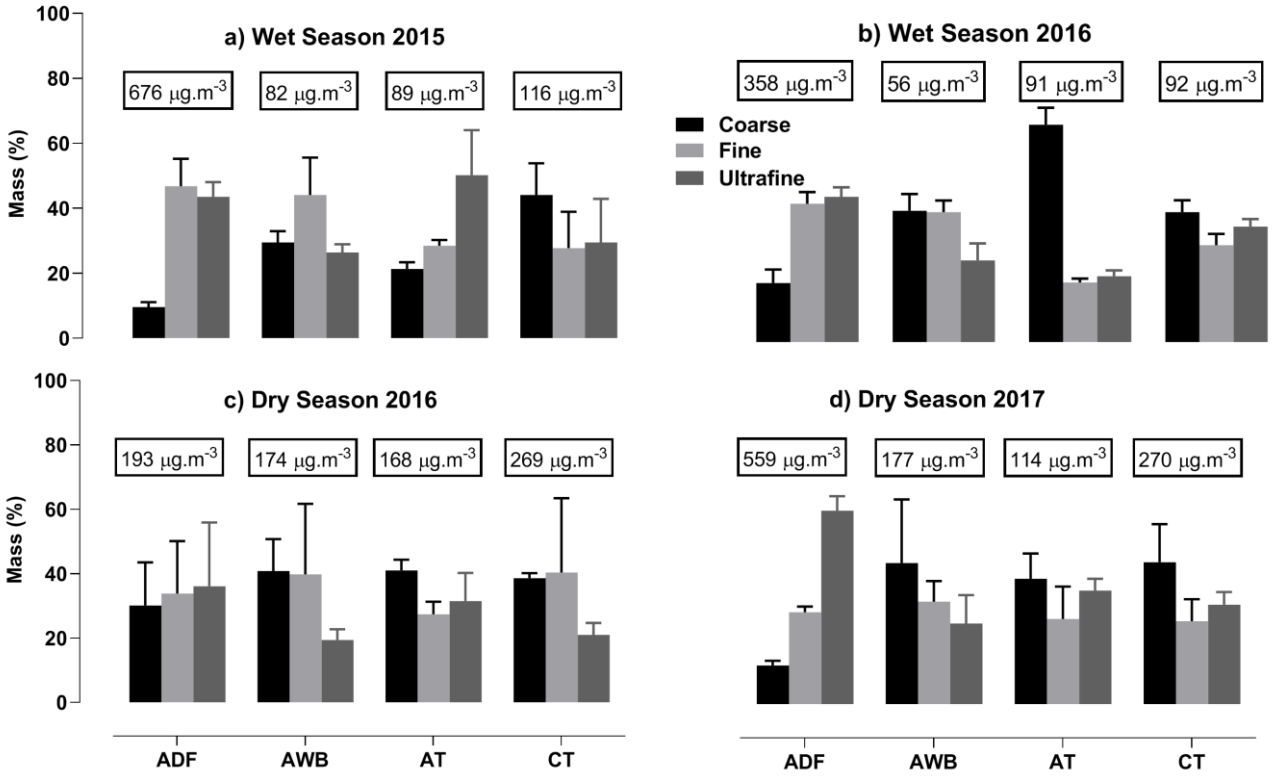
a) Wet Season 2015
676 μg.m-3
82 μg.m-3
89 μg.m-3
116 μg.m-3
b) Wet Season 2016
358 μg.m-3
56 μg.m-3
91 μg.m-3
92 μg.m-3
Coarse
Fine
Ultrafine
c) Dry Season 2016
193 μg.m-3
174 μg.m-3
168 μg.m-3
269 μg.m-3
d) Dry Season 2017
559 μg.m-3
177 μg.m-3
114 μg.m-3
270 μg.m-3
Mass (%)
0
20
40
60
80
100
ADF
AWB
AT
CT

Figure 6

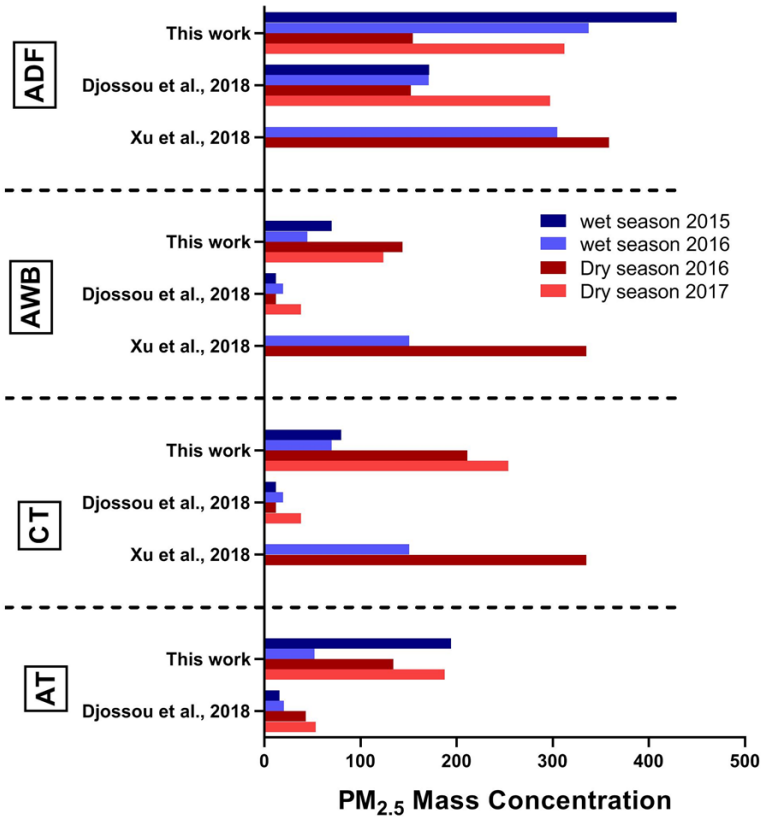
ADF
This work
Djossou et al., 2018
Xu et al., 2018
AWB
This work
Djossou et al., 2018
Xu et al., 2018
CT
This work
Djossou et al., 2018
Xu et al., 2018
AT
This work
Djossou et al., 2018
wet season 2015
wet season 2016
Dry season 2016
Dry season 2017
0
100
200
300
400
500
PM2.5 Mass Concentration

Figure 7

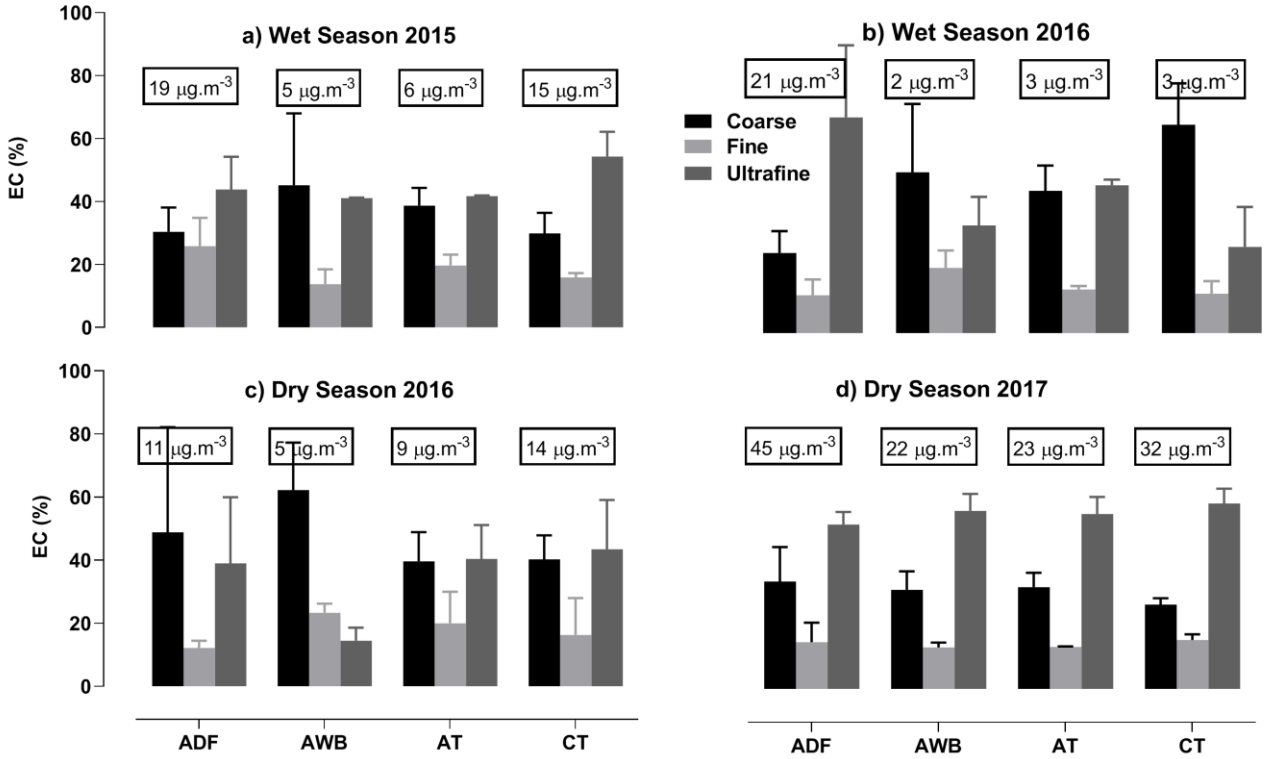
a) Wet Season 2015
b) Wet Season 2016
c) Dry Season 2016
d) Dry Season 2017
EC (%)
Coarse
Fine
Ultrafine
19 µg.m-3
5 µg.m-3
6 µg.m-3
15 µg.m-3
21 µg.m-3
2 µg.m-3
3 µg.m-3
3 µg.m-3
11 µg.m-3
5 µg.m-3
9 µg.m-3
14 µg.m-3
45 µg.m-3
22 µg.m-3
23 µg.m-3
32 µg.m-3
ADF
AWB
AT
CT

Figure 8

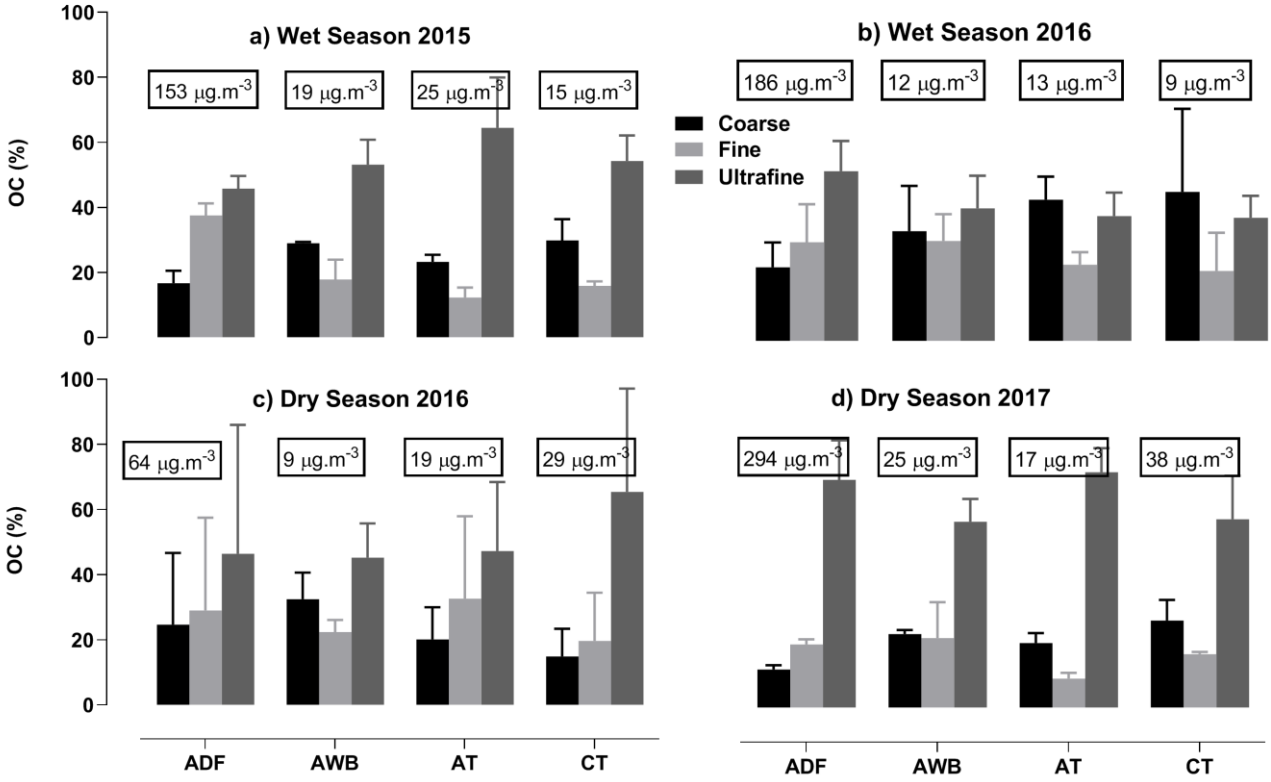
a) Wet Season 2015
b) Wet Season 2016
c) Dry Season 2016
d) Dry Season 2017
OC (%)
153 µg.m-3
19 µg.m-3
25 µg.m-3
15 µg.m-3
186 µg.m-3
12 µg.m-3
13 µg.m-3
9 µg.m-3
64 µg.m-3
9 µg.m-3
19 µg.m-3
29 µg.m-3
294 µg.m-3
25 µg.m-3
17 µg.m-3
38 µg.m-3
Coarse
Fine
Ultrafine
ADF
AWB
AT
CT

Figure 9

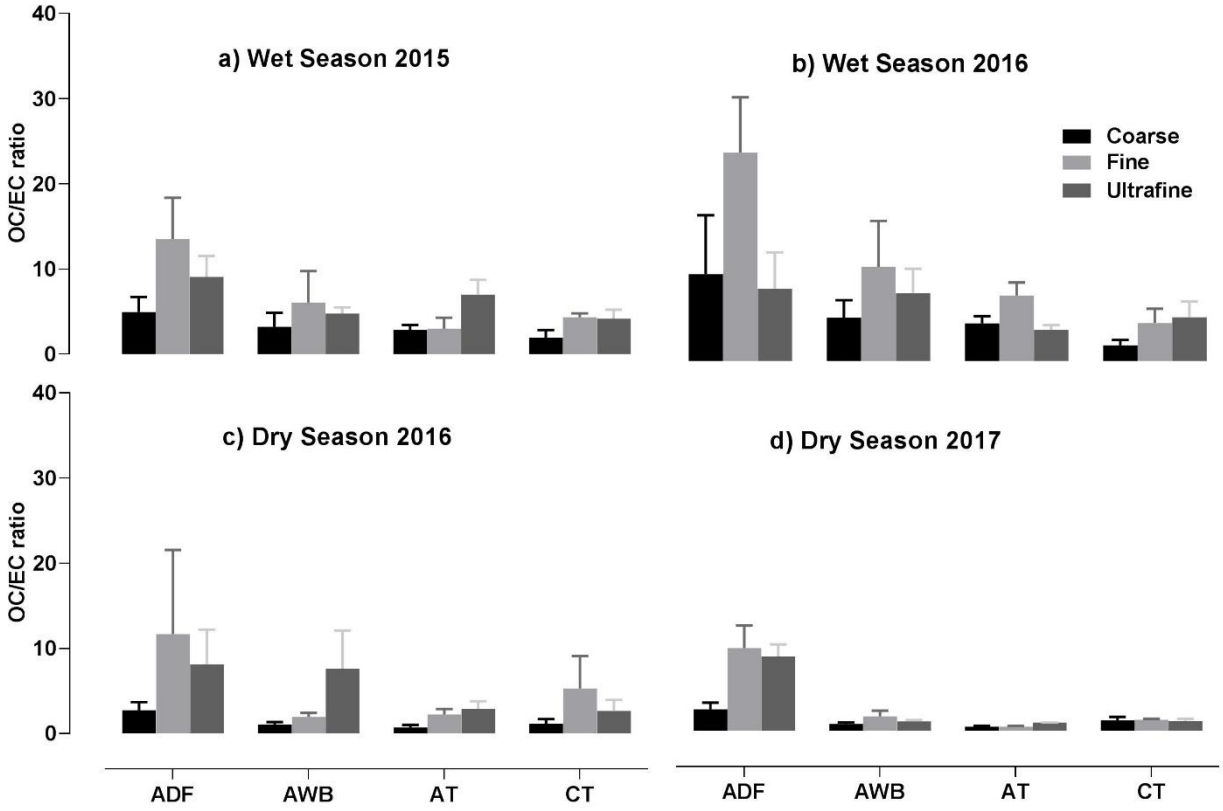

1375

1376 **Figure 10**

1377

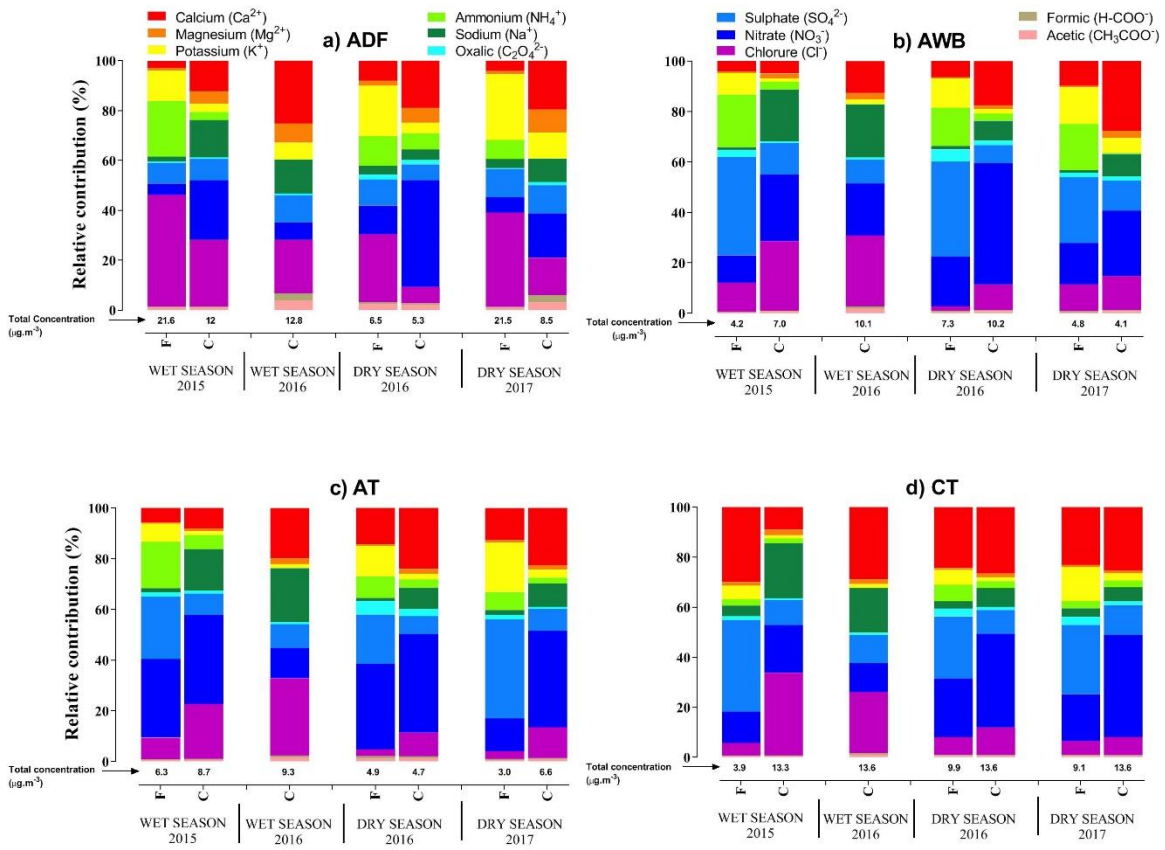
a) ADF
Calcium (Ca^{2+})
Magnesium (Mg^{2+})
Potassium (K^{+})
Ammonium (NH_4^{+})
Sodium (Na^{+})
Oxalic ($C_2O_4^{2-}$)
b) AWB
Sulphate (SO_4^{2-})
Nitrate (NO_3^{-})
Chlorure (Cl^{-})
Formic ($H\text{-}COO^{-}$)
Acetic (CH_3COO^{-})
c) AT
d) CT
Relative contribution (%)
Total Concentration ($\mu g.m^{-3}$)
Total concentration ($\mu g.m^{-3}$)
21.6 12 12.8 6.5 5.3 21.5 8.5
4.2 7.0 10.1 7.3 10.2 4.8 4.1
6.3 8.7 9.3 4.9 4.7 3.0 6.6
3.9 13.3 13.6 9.9 13.6 9.1 13.6
F- C-
WET SEASON 2015
WET SEASON 2016
DRY SEASON 2016
DRY SEASON 2017

Figure 11

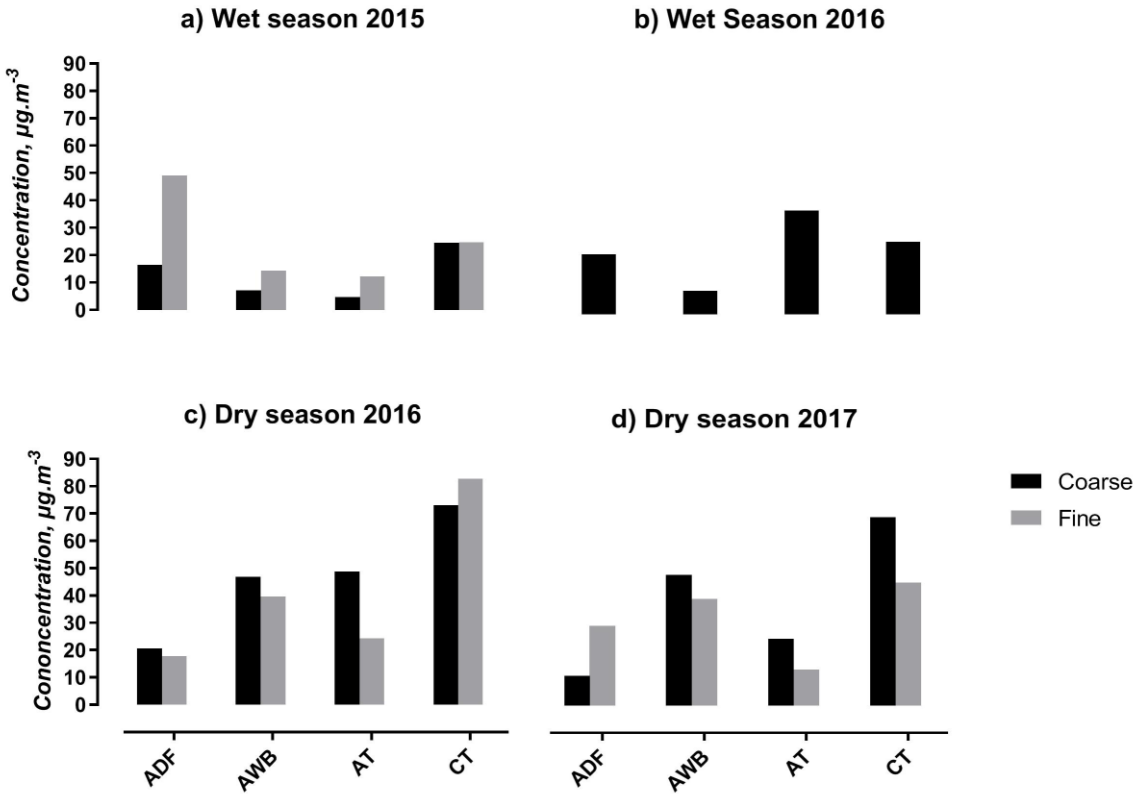

1383

1384 **Figure 12**

1385

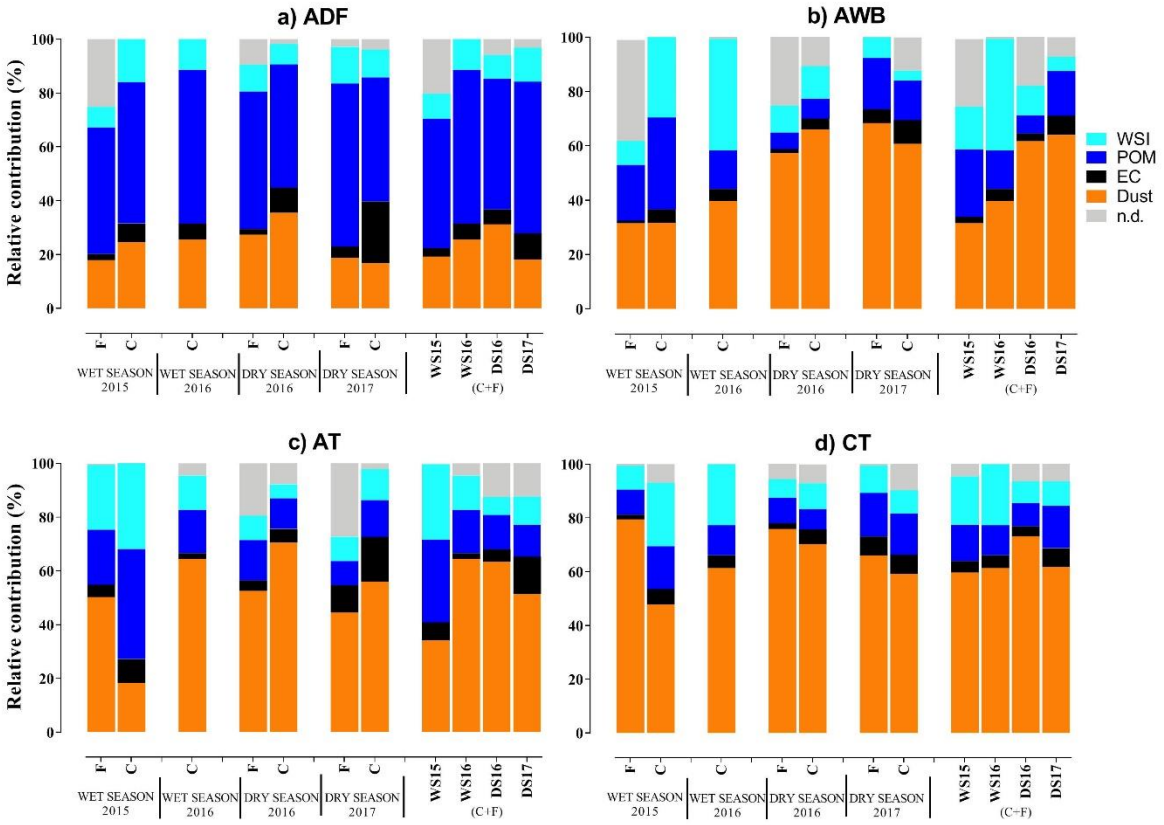
a) ADF
b) AWB
c) AT
d) CT
Relative contribution (%)
WSI
POM
EC
Dust
n.d.
F
C
WET SEASON 2015
WET SEASON 2016
DRY SEASON 2016
DRY SEASON 2017
WS15
WS16
DS16
DS17
(C+F)

Figure 13

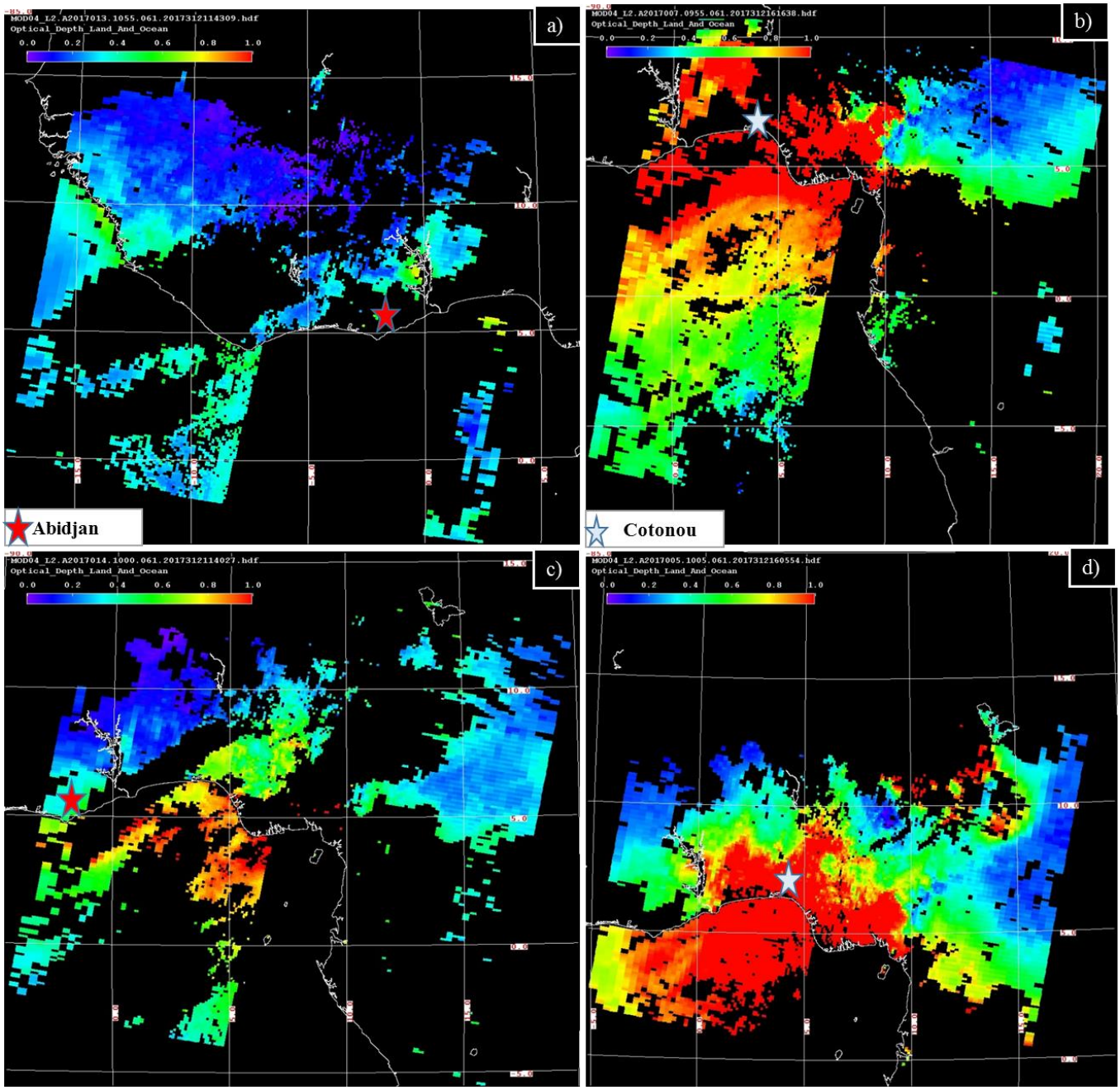

Figure 14

List of table

Table 1: Comparison of dust concentrations obtained from different methodologies in µg.m^{-3}

Dry 2017		**Sciare et al. (2005)**	**Guinot et al. (2007)**	**Terzi et al. (2010)**
ADF	C	18.5	11.2	86.9
	F	9.3	29.7	22.2
	bulk	27.7	40.9	109.1
AWB	C	12.3	48.5	126.4
	F	5.2	39.7	106.4
	bulk	17.6	88.2	232.8
AT	C	16.4	24.8	98.5
	F	4.3	13.4	34.2
	bulk	20.7	38.2	132.7
CT	C	37.9	70.0	98.4
	F	23.4	45.6	55.8
	bulk	61.3	115.6	154.2

Wet 2016		**Sciare et al., 2005**	**Guinot et al., 2007**	**Terzi et al.(2010)**
ADF	C	35.34	21.5	27.9
AWB	C	13.46	8.6	21.1
AT	C	19.65	37.5	21.4
CT	C	42.98	26.2	52.5
	Bulk	42.98	26.2	52.5

1450 Table 2: WSOC concentrations (µg.m^{-3}**)** and WSOC/OC ratios (%) for each site, each campaign and
1451 each aerosol size

Site		**Abidjan Waste Burning**		**Abidjan Domestic Fire**	
Period	**Size**	**WSOC**	**WSOC/OC**	**WSOC**	**WSOC/OC**
Wet season 2015	Coarse	1.3	24,6	8.2	32.5
	Fine	0.7	19.9	12.8	22.7
	Ultra fine	4.1	43.6	51.3	72.5
	PM2.5	5.5	33.7	69.5	47.2
Dry season 2016	Coarse	0.4	12.3	4.4	18.8
	Fine	0.9	46.9	7.0	20.4
	Ultra fine	1.5	38.4	21.9	61.5
	PM2.5	2.7	32.7	31.0	32.0
Wet season 2016	Coarse	1.3	42.5	16.5	44.3
	Fine	0.8	26.3	17.1	33.0
	Ultra fine	2.0	41.2	79.7	84.5
	PM2.5	3.5	37.1	106.0	52.0
Dry season 2017	Coarse	1.9	32.9	12.1	36.0
	Fine	1.4	38.4	19.9	35.0
	Ultra fine	1.6	11.5	38.6	19.0
	PM2.5	4.0	30.0	65.8	29.0

1452

1453

1454 Table 2 (suite): WSOC concentrations (µg.m^{-3}**)** and WSOC/OC ratios (%) for each site, each campaign
1455 and each aerosol size

Site		**Abidjan Traffic**		**Cotonou Traffic**	
Period	**Size**	**WSOC**	**WSOC/OC**	**WSOC**	**WSOC/OC**
Wet season 2015	Coarse	2.4	39.6	1.1	23.3
	Fine	1.3	46.7	0.5	22.1
	Ultra fine	4.7	29.0	0.4	12.7
	PM2.5	6.9	34.0	2.2	18.0
Dry season 2016	Coarse	1.4	43.0	2.3	64.1
	Fine	1.9	59.0	0.6	10.5
	Ultra fine	4.9	62.0	6.3	42.9
	PM2.5	7.5	49.4	8.0	29.0
Wet season 2016	Coarse	1.1	23.1	1.2	34.7
	Fine	0.5	16.8	0.5	32.2
	Ultra fine	1.4	34.8	0.9	23.0
	PM2.5	2.4	26.0	1.9	28.0
Dry season 2017	Coarse	0.9	24.0	3.5	37.8
	Fine	0.3	24.3	2.4	39.6
	Ultra fine	1.8	14.8	1.9	10.4
	PM2.5	2.6	16.0	6.0	18.2

1456 Table 3: Trace element concentrations for bulk aerosol for each site and for DS2017 and WS2016.

	Bulk ng.m^{-3} (%)							
	DRY 2017				WET 2016			
	ADF	**AWB**	**AT**	**CT**	**ADF**	**AWB**	**AT**	**CT**
Al	10050.8 (1.8)	25186.1 (13.7)	14015.8 (12.26)	15480.4 (5.7)	1370.5 (0.4)	1990.1 (3.5)	2191.4 (2.4)	4010.5 (4.4)
K	8634.3 (1.5)	6093.7 (3.3)	3677.7 (3.22)	5068.9 (1.9)	1105.0 (0.3)	472.0 (0.8)	275.9 (0.3)	1076.0 (1.2)
Na	6847.8 (1.2)	23430.5 (12.8)	15372.1 (13.44)	11529.3 (4.3)	2070.6 (0.6)	3735.4 (6.6)	2861.5 (3.1)	5310.2 (5.8)
Ca	4321.2 (0.8)	2923.7 (1.6)	4117.6 (3.60)	6233.5 (2.3)	4124.7 (1.1)	447.5 (0.8)	374.7 (0.4)	4954.02 (5.4
Mg	1940.6 (0.3)	384.0 (0.2)	410.3 (0.36)	823.2 (0.3)	1524.7 (0.4)	294.9 (0.5)	283.5 (0.3)	619.2 (0.7)
Fe	1709.9 (0.3)	3807.9 (2.1)	1628.1 (1.42)	3406.8 (1.3)	1314.0 (0.4)	709.3 (1.3)	987.3 (1.1)	1549.4 (1.7)
P	1521.9 (0.3)	696.0 (0.4)	147.8 (0.13)	207.4 (0.1)	605.4 (0.2)	8.6	13.2	81.4 (0.1)
Ti	488.9 (0.1)	2270.3 (1.2)	282.8 (0.25)	457.9 (0.17)	170.8 (0.05)	75.7 (0.13)	96.8 (0.11)	154.7 (0.17)
Zn	189.7 (0.03)	80.9 (0.04)	57.9 (0.05)	149.4 (0.06)	60.3 (0.02)	1.9	41.1 (0.04)	36.2 (0.04)
Zr	172.1 (0.03)	390.3 (0.21)	217.9 (0.19)	145.3 (0.05)	-	22.4 (0.04)	36.7 (0.04)	31.2 (0.03)
Pb	87.1 (0.02)	11.0 (0.01)	4.8	11.5	8.3	2.1	2.3	9.3 (0.01)
Sn	79.7 (0.01)	38.4 (0.02)	21.6 (0.02)	37.4 (0.01)	0.77	0.09	0.0006	9.ç (0.01)
Mn	74.2 (0.01)	35.2 (0.02)	33.7 (0.03)	160.6 (0.06)	48.9 (0.01)	12.01 (0.02)	9.1 (0.01)	41.41 (0.05)
Rb	52.4 (0.01)	8.7	5.9 (0.01)	8.5	4.47	0.71	0.85	1.9
Sb	59.9 (0.01)	201.2 (0.11)	123.6 (0.11)	149.04 (0.06)	24.4 (0.01)	0	0.0006	2.9
Ba	37.3 (0.01)	53.3 (0.03)	47.4 (0.04)	65.8 (0.02)	18.5	8.02 (0.01)	9.9 (0.01)	32.0 (0.03)
Ni	36.5 (0.01)	34.5 (0.02)	27.9 (0.02)	50.2 (0.02)	18.00)	33.1 (0.06)	9.7 (0.01)	14.9 (0.02)
Cr	29.4 (0.01)	53.8 (0.03)	35.8 (0.03)	28.6 (0.01)	41.9 (0.01)	47.7 (0.08)	24.3 (0.03)	29.7 (0.03)
Sr	28.1 (0.01)	15.5 (0.01)	21.2 (0.02)	34.02 (0.01)	17.02	0	0.19	8.1 (0.01)
Cu	24.0	12.3 (0.01)	3.6	9.6	3.99	0.26	0.87	2.8)
Sr	12.6	-	-	-	17.1	-	0.22	8.9 (0.01)
Li	7.3	15.5 (0.01)	7.8 (0.01)	7.39	0.36	0.32	0.23	0.75
Cd	6.1	1.6	1.0	0.83	1.18	0.05	0.02	0.17
V	5.5	12.4 (0.01)	5.1	10.62	2.14	1.84	2.0	3.35
Mo	5.5	8.0	4.9	3.19	4.56	6.84 (0.01)	2.04	3.2
Cs	5.4	0.9	1.2	0.94	0.11	0.12	0.01	0.17
Hf	4.5	10.8 (0.01)	6.8 (0.01)	4.63	0	0.67	1.03	0.97
As	4.2	4.5	3.1	1.22	0	0 (0)	0.05	0.60
Li	4.0	9.8	5.9 (0.01)	5.82	0.27	0.37	0.16	0.93
Co	3.8	1.1	2.1	35.67 (0.01)	0.86	0.49	0.13	0.33
Ce	3.7	6.8	6.0 (0.01)	9.85	1.06	0.50	0.42	2.03
La	1.8	3.5	2.9	4.78	0.54	0.24	0.25	0.92
Nb	1.5	2.6)	1.4	2.48	0.98	0.46	0.5	0.63
Nd	1.5	2.5	2.4	4.15	0.05	0 (0)	-	0.40
Sc	0.69	1.4	1.1)	1.31		0,00		0.02
Be	0.13	0.19	0.2	0.28	0.003	-	-	0.03
Ga	0.61	1.15	0.8	0.98	0.2	0.11	0.12	0.37
Ge	0.42	1.02	0.8	0.68	0.01	0.07	0.02	0.11
Se	0.91	-	-	0.02	0.59	-	0.20	0.18
Rh	0.02	0.02	0.00002	0.002	-	0.002		0.0002
Te	0.06	0.08	0.08	0.05	0.02	0.02	0.02	0,00
Pr	0.40	0.74	0.7	1.13	0.06	0.01	0.004	0.15
Sm	0.27	0.46	0.45	0.76	0.01	0,00	-	0.07
Eu	0.05	0.08	0.08	0.15	0.01	0.003	-	0.0
Gd	0.31	0.57	0.54	0.86	0.05	0.02	0.001	0.15
Tb	0.04	0.07	0.07	0.10	0.005	-	-	0.02
Dy	0.24	0.42	0.40	0.57	0.001	-	-	0.05
Ho	0.05	0.09	0.09	0.12	0.01	0.008	0.01	0.03
Er	0.16	0.31	0.28	0.35	0.02	0.03	0.02	0.09

Tm	0.02	0.05	0.05	0.05	0.002	0.003	0.001	0.01
Yb	0.18	0.38	0.32	0.34	0.01	0.02	0.03	0.09
Lu	0.03	0.06	0.08	0.06	0.003	0.005	0.005	0.02
Ta	0.07	0.14	0.09	0.16	0.06	0.02	0.02	0.03
W	0.80	1.63	0.69	0.54	0.26	0.41	0.4	0.3
Tl	0.22	0.01	0.03	0.06		0.009		
Bi	0.32	0.26	0.02	0.08	0.06	-	-	0.08
Th	0.41	0.88	0.79	1.29	0.15	0.09	0.09	0.24
U	0.22	0.43	0.49	0.51	0.03	0.03	0.02	0.09
Total	36459.9	65817.6	40312.2	44159.2	12562.9	7874.7	7227.2	18001.1
Mass(µg/m^3)	558.8	183.6	114.4	270.0	374.7	56.3	91.6	91.9

Table 4: Comparison of PM2.5 concentrations with literature data. Only literature data given at a daily scale have been selected.

Location	PM2.5 ($\mu g.m^{-3}$)	Reference
Abidjan, Côte d'Ivoire	142	This work
Cotonou, Benin	154	This work
Beijing, China	81.4	Xie et al., 2019
Christchurch, New Zealand	9.2	Tunno et al., 2019
Pune, India	98 ± 28	Pipal et al., 2019
Delhi, India	123	Guttikunda and Calori, 2013
Lahore, Pakistan	91	Colbeck et al., 2011
Ahvaz, Iran	69	Shahsavani et al., 2012
Hong Chong, Hong Kong	54.7 ± 25.6	Cheng et al., 2015
Lecce, Italia	16	Cesari et al., 2016
Libreville, Gabon	35.8	Ngo et al., 2019
Port Gentille, Gabon	60.9	
Kenitra, Morocco	51.3	Zghaid et al., 2009
Bilecik, Turkey	247	Gaga et al., 2018
Algiers, Algeria	34.8	Bouhila et al., 2015
Shobra, Egypt	216	Lowenthal et al.,2015

Table 5: PM2.5-EC and PM2.5-OC comparison with Djossou et al. (2018) and Xu et al. (2019) values. Units are µgC.m^{-3}.

Location	Period	PM2.5 OC	PM2.5 EC	References
Traffic Abidjan. Cote d'Ivoire	July 2015	22.6 ± 3.4	4.3 ± 0.2	This Work
	January 2016	15.2 ± 5.3	7.0 ± 2.6	
	July 2016	9.3 ± 1.3	2.2 ± 0.1	
	January 2017	16.1 ± 1.7	18.9 ± 1.4	
	July 2015	3.3 ± 0.2	2.3 ± 0.2	Djossou et al. 2018
	January 2016	7.7 ± 0.0	3.9 ± 0.0	
	July 2016	7.6 ± 0.2	4.9 ± 0.0	
	January 2017	19.1 ± 6.2	13.9 ± 5.5	
Traffic Cotonou. Benin	July 2015	13.1 ± 1.2	3.5 ± 0.7	This Work
	January 2016	27.8 ± 11.3	10.9 ± 2.6	
	July 2016	6.7 ± 1.9	2.0 ± 0.5	
	January 2017	33.1 ± 4.6	27.3 ± 0.9	
	July 2015	4.2 ± 0.7	1.5 ± 0.1	Djossou et al. 2018
	January 2016	3.0 ± 0.3	1.5 ± 0.2	
	July 2016	6.7 ± 0.2	1.6 ± 0.1	
	January 2017	14.5 ± 0.8	4.4 ± 0.7	
	January 2016	49.5 ± 12.5	13.6 ± 3.6	Xu et al. 2019
	July 2016	37.0 ± 3.5	9.3 ± 0.8	
Domestic fire Abidjan. Cote d'Ivoire	July 2015	147.2 ± 14.5	16.1 ± 1.6	This Work
	January 2016	56.5 ± 51.5	7.4 ± 3.1	
	July 2016	172.3 ± 39.0	17.9 ± 4.8	
	January 2017	283.9 ± 34.9	37.9 ± 4.3	
	July 2015	80.5 ± 1.1	32.2 ± 1.6	Djossou et al. 2018
	January 2016	76.3 ± 13.7	11.4 ± 0.2	
	July 2016	68.4 ± 16.5	17.4 ± 2.1	
	January 2017	66.4 ± 7.5	21.1 ± 6.6	
	January 2016	72.4 ± 24.6	19.5 ± 7.3	Xu et al. 2019
	July 2016	189.3 ± 197.8	11.5 ± 10.8	
Waste Burning Abidjan. Cote d'Ivoire	July 2015	14.8 ± 1.1	4.4 ± 0.1	This Work
	January 2016	7.7 ± 1.3	3.0 ± 0.3	
	July 2016	10.0 ± 2.4	1.5 ± 0.3	
	January 2017	21.9 ± 4.2	19.2 ± 2.4	
	July 2015	3.7 ± 2.2	4.3 ± 0.3	Djossou et al. 2018
	January 2016	13.9 ± 9.0	3.6 ± 1.8	
	July 2016	9.8 ± 4.4	2.8 ± 0.9	
	January 2017	22.4 ± 7.8	8.7 ± 3.0	
	January 2016	85 ± 57.4	15 ± 4.7	Xu et al. 2019
	July 2016	65.2± 65.2	12.3 ± 11.4	

Table 6: EC and OC comparison with literature values. Only literature data given at a daily scale have been selected.

Location	**OC (µg.m^{-3})**	**BC (µg.m^{-3})**	**Reference**
Abidjan (Côte d'Ivoire)	16	8.1	This study
Cotonou (Benin)	20.2	11	This study
Bilecik (Turkey)	49.6-62.8	38.8-58.1	Gaga et al., 2018
Pune (India)	30	5	Pipal et al., 2019
Shanghai (China)	4.9-13.1	1.9-5	Ding et al., 2017
Lahore (Pakistan)	85.7-152	13.8-21	Stone et al., 2010
Agra (India)	25.4-70	3.3-9.5	Satsangi et al., 2012, Pipal et al., 2014
Delhi (India)	34.1-50	5.3-10.6	Bisht et al., 2015a, Pipal et al., 2014
Ahmedabad (India)	18.3	3	Rengarajan et al., 2011
Yokohama (Japan)	4	2	Khan et al., 2010
Beijing (China)	2.9-28.2	1.2-16.3	Guinot et al., 2007

Table 7: Comparison of WSOC concentrations with literature data. Only literature data given at a daily scale have been selected.

Location	**WSOC (µg.m^{-3})**	**Reference**
Abidjan, Côte d'Ivoire	2-8	This work
Cotonou, Benin	2-8	This work
Beijing, China	9-27	Yu et al., 2018
Beijing, China	4-6	Xiang et al., 2017
Beijing, China	8-12	Tang et al., 2016
Beijing, China	7	Du et al., 2014
Beijing, China	6-8	Feng et al., 2006
Shanghai, China	2-7	Feng et al., 2006, Huang et al., 2012
Guangzhou, Hong Kong	2	Huang et al., 2012
Guangzhou, Hong Kong	5-10	Feng et al., 2006
Gwangju, Korea	2-3.5	Park et al., 2015
Tokyo, Japan	3-23	Sempere and Kawamura, 1994
Cairo, Egypt	3	Favez et al., 2008
Amsterdam, Netherland	1-2	Feng et al., 2007
Barcelone, Spain	1-2	Viana et al., 2007 and 2008
Brindisi, Italy	1.5	Genga et al., 2017
Saint Jean de Maurienne, France	1-5	Sullivan et al., 2004, Jaffrezo et al., 2005a